International Journal of Nanomedicine

Dovepress
Taylor & Francis Group

Open Access Full Text Article

ORIGINAL RESEARCH

Human Schwann Cell-Derived Extracellular Vesicle Isolation, Bioactivity Assessment, and Omics Characterization

Aisha Khan[1,2], Julia Oliveira[2], Yee-Shuan Lee[1], James D Guest[2,3], Risset Silvera[2], Yelena Pressman[2], Damien D Pearse[2,3], Adriana E Nettina[1,2], Pascal J Goldschmidt-Clermont[4], Hassan Al-Ali[2], Indigo Williams[2], Allan D Levi[2,3], W Dalton Dietrich[2,3]

[1]Interdisciplinary Stem Cell Institute, Miller School of Medicine, University of Miami, Miami, FL, USA; [2]The Miami Project to Cure Paralysis, Miller School of Medicine, University of Miami, Miami, FL, USA; [3]Neurological Surgery, Miller School of Medicine, University of Miami, Miami, FL, USA; [4]Miller School of Medicine, University of Miami, Miami, FL, USA

Correspondence: Aisha Khan, Email akhan@med.miami.edu

Purpose: Schwann cell-derived extracellular vesicles (SCEVs) have demonstrated favorable effects in spinal cord, peripheral nerve, and brain injuries. Herein, a scalable, standardized, and efficient isolation methodology of SCEVs obtaining a high yield with a consistent composition as measured by proteomic, lipidomic, and miRNA analysis of their content is described for future clinical use.

Methods: Human Schwann cells were obtained ethically from nine donors and cultured in a defined growth medium optimized for proliferation. At confluency, the culture was replenished with an isolation medium for 48 hours, then collected and centrifuged sequentially at low and ultra-high speeds to collect purified EVs. The EVs were characterized with mass spectrometry to identify and quantify proteins, lipidomic analysis to assess lipid composition, and next-generation sequencing to confirm miRNA profiles. Each batch of EVs was assessed to ensure their therapeutic potential in promoting neurite outgrowth and cell survival.

Results: High yields of SCEVs were consistently obtained with similar comprehensive molecular profiles across samples, indicating the reproducibility and reliability of the isolation method. Bioactivity to increase neurite process growth was confirmed in vitro. The predominance of triacylglycerol and phosphatidylcholine suggested its role in cellular membrane dynamics essential for axon regeneration and inflammation mitigation. Of the 2517 identified proteins, 136 were closely related to nervous system repair and regeneration. A total of 732 miRNAs were cataloged, with the top 30 miRNAs potentially contributing to axon growth, neuroprotection, myelination, angiogenesis, the attenuation of neuroinflammation, and key signaling pathways such as VEGFA-VEGFR2 and PI3K-Akt signaling, which are crucial for nervous system repair.

Conclusion: The study establishes a robust framework for SCEV isolation and their comprehensive characterization, which is consistent with their therapeutic potential in neurological applications. This work provides a valuable proteomic, lipidomic, and miRNA dataset to inform future advancements in applying SCEV to the experimental treatment of neurological injuries and diseases.

Keywords: myelination, axon growth, neuroprotection, regeneration, lipidomic

Introduction

The mammalian nervous system has a limited capacity to recover after an injury, either triggered by neurological illness or trauma. While peripheral nervous system regeneration can be partially achieved in some cases, the central nervous system fails to regenerate.[1] Glial cells are one of the several factors responsible for the differences in the regeneration response between both systems. The main glia of the peripheral nervous system is the Schwann cell (SC), which has unique features that contribute to axonal repair by several means,[2] including myelinophagy,[3] transfer of lactate,[4] iron,[5] and ribosomes,[6] the release of neurotrophic factors,[7,8] production of basal lamina,[9] remyelination,[10] and the release of extracellular vesicles (EVs).[11,12]

Received: 10 October 2024
Accepted: 5 February 2025
Published: 4 April 2025

The transplantation of cultured autologous SC (aSC) for treating neurological conditions has shown benefits.[13–19] However, aSC cultures have significant limitations, including limited mitotic capacity in vitro, time required for product preparation, and immunological responses to allogeneic transplants.[20] SC-derived extracellular vesicles (SCEVs) may avoid most of these limitations of aSC transplantation, especially in manufacturing an allogeneic off-the-shelf product for clinical applications.[21]

EVs are nano-sized, membrane-bound particles rich in proteins, lipids, nucleic acids, and metabolites released by cells into the extracellular environment.[22] They play crucial roles in cell-to-cell communication, tissue repair, and the modulation of biological processes.[23] Among the potential sources of EVs, those derived from SC resembling the repair phenotype[14,24] hold particular therapeutic promise.[13,25–27] Recent advances have highlighted SCEVs as key mediators of regenerative processes, carrying a cargo rich in regenerative and anti-inflammatory molecules capable of promoting neuronal survival, axonal growth, and remyelination.[28–30] The therapeutic potential of these SCEVs could extend to peripheral nerve injuries (PNI), spinal cord injury (SCI), traumatic brain injury (TBI), and neurodegenerative diseases, including amyotrophic lateral sclerosis (ALS), and potentially beyond, to disorders involving other systems where SC signaling plays a reparative role.[31–33] These vesicles, carrying myriad bioactive molecules, can potentially transform how we approach treating neurological injuries and diseases.[34] In addition to their therapeutic potential,[21,35] our group demonstrated that weekly intravenous infusion of allogeneic human SCEVs for ten weeks in one patient with ALS was safe and correlated with clinical stabilization of the ALS Functional Rating Scale-Revised (ALSFRS-R) and pulmonary function.[11,36]

The exploration of EVs as carriers of therapeutic agents represents a frontier in regenerative medicine, with SCEVs exhibiting unique reparative properties.[21] These vesicles could lead to a novel class of biological therapeutics capable of harnessing the body's own mechanisms for repair and regeneration.[13–15,18,21,37,38] Although many studies have examined the regenerative potential of SCEVs,[21,35] we found only one study of the proteome of rat SCEVs.[39]

The molecular characterization of human SCEVs is not well understood. By exploring their content, our study aimed to advance the understanding of SCEVs' biology and possible molecular mechanisms that can facilitate the discovery of novel therapeutic targets[40] for intervention in specific neurological injuries and diseases. In this paper, we show that human SCEVs promote neurite outgrowth of rat hippocampal neurons in vitro and provide a molecular profile through proteomic, lipidomic, and miRNA analysis focused on their neuroregenerative potential for future exploration in well-defined indication of diseases.

Materials and Methods

Sural Nerve Sourcing, Donor Qualification, and SC Culture

Human SC were obtained from the sural nerves of nine cadaveric donors as described previously for both research and clinical batches.[18] Donor screening followed standard transplant practices, and all allogeneic donors met allogeneic donor eligibility criteria as outlined in FDA's 21 CFR Part 1271 for cadaveric donors[41] regarding testing for infectious agents and source documentation.

Human sural nerve were transported in a sterile tissue container with approximately 100 mL of Belzer UW® cold storage solution (Bridge to Life Ltd, Northbrook, IL, USA) at 2 to 10°C, and sterility (aerobic, anaerobic, and fungal culture) testing was performed. Fascicles were pulled from nerves, transferred to a T-75 flask (Corning, Corning, NY, USA), and cultured with Schwann cell growth (SCG) media. SCG media was composed of 10% FBS (Hyclone, Marlborough, MA, USA), 2 µM forskolin (Sigma, St Louis, MO, USA), 10 nM Heregulin ß-1 (PeproTech, Cranbury, NJ, USA), 4 mM L-glutamine (Invitrogen, Waltham, MA, USA), 0.05 mg/mL Gentamicin USP grade, and DMEM (Invitrogen, Waltham, MA, USA). SCG media was changed every other day, and fascicles were incubated overnight with a dissociation enzyme solution after 7 or 8 days. The cell suspension from the dissociated fascicles was washed and cultured with SCG media in laminin (Sigma, St Louis, MO, USA)-coated T-75 flasks (Corning, Corning, NY, USA). Culture media was changed every three days, and the SCs were harvested when they reached confluency. The SC were then cultured for further expansion on laminin-coated flasks or cryopreserved for further expansion. The culture process followed previously published manufacturing methods for clinical-grade Schwann cells[11,13–15,17–19,36] and is summarized

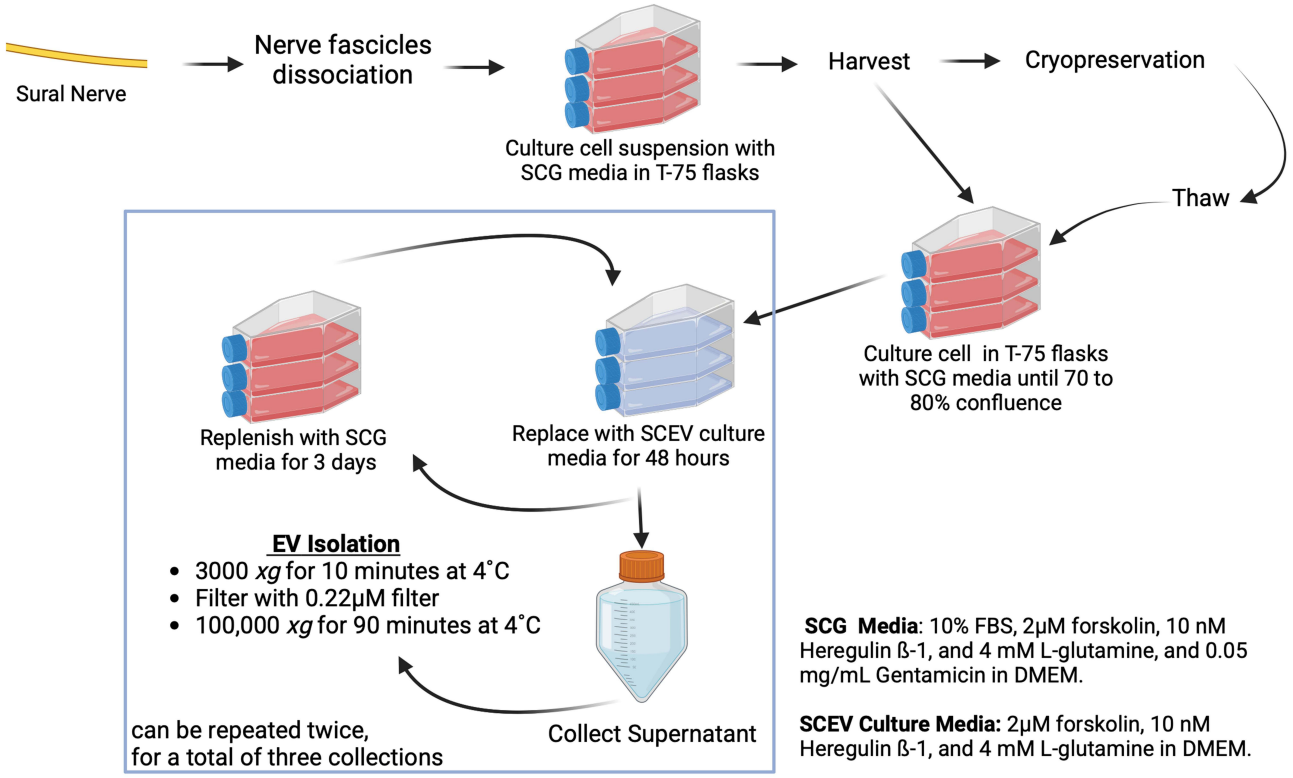

Figure 1 Manufacture Process of SCs and SCEVs. Starting with sural nerve tissue, cells are dissociated, cultured in T-75 flasks to 70–80% confluence, and either cryopreserved or further cultured. Post-culture, the SCG medium is replaced with SCEV culture media to induce EV production. The supernatant is collected and processed through sequential centrifugation and filtration to isolate EVs. The procedure permits up to three EV harvests.

in Figure 1. Research batches were produced in a regular research laboratory setting, whereas the clinical batches were produced in a clean environment following cGMP using the same methodology.

Isolation and Purification of SCEVs

When SC reached 70 to 80% confluence in the flasks, the SCG medium was removed. Flasks were rinsed with DPBS twice before being replenished with SCEV serum-free culture media, composed of DMEM (Invitrogen, Waltham, MA, USA) 2µM forskolin (Sigma, St Louis, MO, USA), 10 mm Heregulin ß-1 (PeproTech, Cranbury, NJ, USA), 4 mm L-glutamine (Invitrogen, Waltham, MA, USA). The supernatant was collected 48 hours later, and the flasks were replenished with SCG medium. The SCs were cultured with SCG medium for another 3 days, then rinsed with DPBS (Gibco, Grand Island, NY, USA) twice then replenished with SCEV serum-free culture medium. Forty-eight hours later, the supernatant was collected, and the flasks were replenished with SCG medium. This process was repeated once more for a total of three collections of supernatants (summarized in Figure 1). The supernatant was centrifuged at 3000 *x g* for 10 minutes at 4°C, then filtered with a 0.22 µM cellulose acetate filter (Corning, Corning, NY, USA). The filtered supernatant was then centrifuged at 100,000 *x g* for 90 minutes at 4°C using Optima XPN-90 ultracentrifuge (Beckman Coulter, Brea, CA, USA). After removing the supernatant, the SCEVs were resuspended with DPBS (Gibco, Grand Island, NY, USA), then aliquoted and stored at −80°C.

Transmission Electron Microscopy

EV samples from the research batches were prepared for transmission electron microscopy. They were loaded onto a carbon copper grid for 30 minutes and then rinsed with phosphate buffer, followed by double-distilled water. The samples were then fixed with 2% glutaraldehyde and stained with 2% aqueous uranyl acetate solution. Grids were kept overnight protected from light and were viewed at 80 kV in a JEM-1400 transmission electron microscope (JEOL LTD, Peabody, MA, USA), where images were captured with an AMT BioSprint 12 digital camera.

https://doi.org/10.2147/IJN.S500159

Total Protein Analysis

EV samples from research and clinical batches were prepared to analyze total protein content using a DC Protein Assay Kit (Bio-Rad Laboratories, Hercules, CA, USA). In brief, μL of purified EV samples were added to the reagent A (alkaline copper tartrate solution) and mixed well. Then, reagent B (dilute Folin reagent) was added and mixed, and the mixture was incubated at room temperature for 15 minutes. Absorbance was measured at 750 nm.

Nanoparticle Tracking Analysis (NTA)

EVs were diluted with distilled water to a final volume of about 1 mL for NTA using NanoSight NS300 (Malvern Panalytical, Malvern, UK). For each measurement, the ideal particle per frame was between 30 and 60 for each 30 seconds of capture for five captures. The camera capture level was between 13 and 15, with a syringe speed of 30 μL/s. After capture, the videos were analyzed using the built-in NanoSight Software 3.4 with a detection threshold of 5.

Phenotype Analysis

EVs were incubated with CD63 Isolation magnetic beads (Invitrogen, Waltham, MA, USA) overnight at 4°C and then incubated with conjugated antibodies for exosome surface markers against CD63-FITC (BD Biosciences, Franklin Lakes, NJ, USA), CD81-PE (BD Biosciences, Franklin Lakes, NJ, USA), and CD9-PE (BD Biosciences, Franklin Lakes, NJ, USA) for one hour at room temperature. The EVs were rinsed once and then analyzed using a Cytoflex Flow cytometer (Beckman Coulter, Brea, CA, USA).

Neurite Growth Assay of Hippocampal Neurons

The assays followed published methods.[23] In brief, embryonic hippocampal neurons from E18 Sprague-Dawley rats were plated at 2000 cells per well on a poly-D-lysine coated 96-well plate with 150 μL NbActiv4 media (BrainBits, Springfield, IL, USA) for 1 hour at 37°C and 5% CO_2. The procedures for neuron extraction were approved by the Animal Care and Use Committee of the University of Miami (protocol # 21–138) and following USDA and AAALAC guidelines for animal welfare. Eight research batches of exosomes were tested, either with 6×10^9 or 6×10^{10} particles/mL. The control groups were treated with 0 or 10 ng/mL of NGF. The hippocampal neurons were cultured for a further 48 hours, then fixed with 4% paraformaldehyde (Sigma, St. Louis, MO, USA) and permeabilized with 0.3% Triton-X solution (Millipore, Burlington, MA, USA) for 1 hour, followed by blocking with 0.03% Triton-X, 0.2% fish gelatin (Sigma-Aldrich, St. Louis, MO, USA), 2% sodium azide (Sigma-Aldrich, St. Louis, MO, USA) in PBS for 1 hour at room temperature. Cultures were stained with rabbit anti-ßIII-tubulin antibody (Sigma-Aldrich, St. Louis, MO, USA, 1:2000) overnight at 4°C, then washed 5 times with PBS. The secondary antibody (Thermo Fischer, Waltham, MA, USA, 1:1000) with 10 μM Hoescht (Invitrogen, Waltham, MA, USA) was added to each well and incubated for 1 hour at room temperature, then each well was washed 5 times with PBS before being imaged using Opera Phenix High-Content Screening System (Revvity, Waltham, MA, USA). Nine fields were imaged with a 10X objective for each well and analyzed automatically using the neurite tracing algorithm implemented in Harmony v5.1 (high-content imaging and analysis software, Revvity, Waltham, MA, USA), and the total neurite length was assessed.

Preparation of EV Samples for RNA-Seq, Proteomic, and Lipidomic Analysis

Two research batches and one clinical batch of SCEVs were sent to Creative Biolabs (Shirley, NY, US) for sample preparation and processing for RNA-seq, proteomic, and lipidomic analysis. The samples were labeled as hSCExo1(R), hSCExo2(R) as research batches and hSCExo3(C) as clinical batch. This labeling is part of sample traceability, ensuring that each cell batch can be tracked through its source, handling, and experimental use.

SCEVs isolated from three human donors were lysed to release RNA. This RNA was then extracted using the exoRNeasy Serum/Plasma Maxi Kit (Qiagen, Germantown, MD, USA), specifically designed for high-yield and purity RNA extraction from such samples. The extracted RNA was used to synthesize cDNA for the subsequent analysis. The cDNA samples were then sequenced using the Illumina platform with a PE150 sequencing strategy wherein paired end reads of 150 base pairs each were generated, allowing for comprehensive and detailed sequencing coverage. The RNA

sequencing data was processed using Seqtk (single-threaded), a tool for manipulating sequences in the FASTQ format. This included removing any linker sequences and trimming sequences where the base quality at the 3' end was below a Q-score of 20, ensuring that only high-quality, error-free reads (error rate less than 0.01) were analyzed.

Protein was extracted, and the concentration was determined using a bicinchoninic acid (BCA) assay. Desalinization and freeze-drying were performed before analyzing the sample with Mass spectrometry. An ORBITRAP ELIPE mass spectrometer with a Nanospray Flex^{TM} ion source was used at 2.0 kV. The full scan range was 350 to 1500 m/z at 120000 resolutions. Raw Mass Spectrometry files were processed using Proteome Discoverer Software (version 2.4.1.15) and searched in the UniProt database (uniprot.org).

Lipids from exosome samples were isolated using chloroform (Sigma-Aldrich, St. Louis, MO, USA) and methanol (2:1, v/v) at −20°C and processed to a freeze-dried sample. The sample was then resuspended in 200 µL of isopropanol and analyzed by Mass spectrometry. Spray voltages of 3.5 kV and 2.5 kV were used, and the full scan range was set to 150 to 2000 m/z at 35000 resolutions. LipidSearch (V4.2.28) was used to annotate the original data, and peak alignment and peak filtering were performed.

Analysis of miRNA, Proteomic, and Lipidomic Data

All analyses were performed using the raw data processed and collected by Creative Biolabs. The detected miRNAs were filtered to consider only those concordant in at least 2 out of the 3 samples. The raw intensity levels of proteins and lipids were normalized to the mean Z-score, and the miRNA sequence depth was normalized by counts per million. For overlap analysis among samples, Venn diagrams with all identified lipids, proteins, and miRNA in all three samples were generated using an online tool.[42] The Pearson correlation coefficient was utilized to analyze the correlation of intensity levels among samples, and heatmaps were plotted using the corrplot package in RStudio (Posit, PBC, version 2023.12.1–402).

For profile analysis, normalized data for each detected miRNA, lipid, and protein in each sample was pooled by mean and ultimately ranked by expression levels. The top 30 miRNAs and their corresponding potential influence on nervous system regeneration were searched in the literature (PubMed database) and listed in a table containing each miRNA and its respective role, study model, and mechanism of action. Target gene prediction analysis of the top 30 miRNAs was performed using the interactive online tool Mienturnet[43] and selecting the miRtarBase database.[44] A false discovery rate (FDR) below 0.05 was considered, and one was set as the threshold for the minimum number of miRNA-target interactions. The resulting list was plotted as an interaction network using Cytoscape (Cytoscape Team, v.3.10.2).

Proteomic analysis was conducted by ranking all the detected 2517 proteins based on intensity levels, followed by selecting the 1259 proteins that presented expression levels above the median and submitting them to the gene list to the Database for Annotation, Visualization, and Integrated Discovery (DAVID, version 2021)[45] for functional enrichment analysis. For identifying enriched biological themes, we selected the following functional annotation tools: the Kyoto Encyclopedia of Genes and Genomes (KEGG), Wikipathways, Reactome, Gene Ontology molecular function (MF) and biological process (BP), and UniProt. Functional terms related to nervous system regeneration with a false discovery rate (FDR) below 0.05 were filtered, ranked, and listed in a table.

The lipidomic analysis was performed by counting the total number of lipid molecules per lipid subclass identified, represented by the bar graph generated in Microsoft Excel (version 16.78), and by the percentage of lipid subclass identified, represented by the doughnut graph.[46]

Safety Determination: Sterility, Mycoplasma, and Endotoxin

Clinical batch samples were subjected to bacterial (aerobic and anaerobic) and fungal testing. For these tests, the membrane filtration method was employed in accordance with the procedures outlined in 21 CFR Part 610.12 (6) (US Food and Drug Administration, 2023c) and/or the current United States Pharmacopeia.[47] Sterility testing involves using Soybean-Casein Digest (SCD) and Fluid Thioglycollate Media (FTM) and cultures of aerobic, anaerobic, and fungal organisms using media selective to the respective types of organisms. Samples were incubated for 14 days. For Mycoplasma, samples were tested by PCR amplification using the VenorGeM® Mycoplasma Detection Kit (Sigma-Aldrich, St. Louis, MO, USA). This method can detect 1–5 fg of Mycoplasma DNA corresponding to 2–5 Mycoplasma

per sample volume for detection. For endotoxin, samples were tested by Limulus Amebocyte Lysate (LAL) using the Endosafe®-PTS portable test system (Charles River, Wilmington, MA, USA). The Endosafe®-PTS is an FDA-Licensed Endotoxin detection system that utilizes a LAL test cartridge along with a handheld spectrophotometer to provide point-of-use results. PTS system uses LAL kinetic chromogenic technology that measures a color intensity that is directly correlated to the Endotoxin concentration in a sample.

Statistical Analysis

For EV Mode size, particle concentration, and protein levels of phenotypical markers (CD63, CD81, and CD9) that were normally distributed and analyzed using unpaired t-tests comparing research and clinical batches. Neurite outgrowth was normally distributed and analyzed through one-way ANOVA with Tukey's multiple comparisons test. Both tests were performed using GraphPad Prism (Prism 10.3.1 for macOS), and a significant difference was defined as $p<0.05$.

Results

Reproducibility of SCEVs Among Various Donors

We utilized the described methods to produce 25 research batches from seven donors and 6 clinical batches from two donors included in this study. The release testing for both the research and clinical batches of SCEVs is detailed in Table 1. A typical TEM image of SCEV is shown in Figure 2A. Detailed product characterization for the research SCEVs batches is provided in Table 2, and for the clinical SCEVs batches in Table 3. The manufacturing method did not differ between research and clinical batches. However, clinical batches were produced in compliance with cGMP and underwent additional testing for sterility and mycoplasma to meet regulatory standards (Table 1).[47–49]

The average mode size was 128.1±11.4 nm for research batches and 107.12±10.4 nm for clinical batches (Figure 2B). The average of clinical batches was significantly smaller ($p<0.05$) in mode size than in the research batches. The average concentration was $6.01x10^{11}±3.22x10^{11}$ particles/mL for research batches and $5.52x10^{11}±4.18x10^{11}$ particles/mL for clinical batches (Figure 2C), showing no significant differences. The average total protein yield for research SCEVs was 0.34 mg/mL, and for clinical SCEVs, it was 0.36 mg/mL, with no significant differences. The average CD63, CD81, and CD9 expression was 71.18%, 76.80%, and 76.95%, respectively, for research batches and 96.28%, 90.67%, and 92.20% for clinical batches (Figure 2D). The average CD63 and CD81 expression in the research batches was significantly lower ($p<0.05$ for both) than in the clinical batches.

In the clinical SCEV batches, there were two donors, one 22-year-old male and one 45-year-old female (Table 3), while in the research SCEV batches, there are seven donors, ages ranging between 12 and 50, including both females and males (Table 2). The large number of donors in the research batches of SCEVs contributed to the greater variation in particle mode size and phenotype than in clinical batches. One research SCEV research batch run yielded low phenotype expression across all three markers, while the rest of the research SCEV batches showed similar phenotypical expression. No clear trends were observed in relation to the age (Figure 2E) of the donors of SCs used for research batches SCEV production and phenotype distribution. Research batches of SCEVs produced from male donors seemed to be clustering

Table 1 Release Testing Summary of Research and Clinical Batches SCEVs. This Table Delineates the Specific Testing Parameters and Release Specifications Set for Both Research and Clinical Batches, Ensuring Quality Control and Consistency Across Different Stages of Production

Testing	Release Specification	Research Batch	Clinical Batch
Phenotype Analysis (by flow cytometry)	CD81>80% CD63>80%	Tested	Tested
Particle Mode Size and Concentration (by Nanosight)	Particle Mode size between 50 to 200 nm	Tested	Tested
Total Protein	N/A	Tested	Tested
Sterility (Aerobic, anaerobic, and fungal)	Negative	*Not Tested	Tested
Mycoplasma	Negative	*Not Tested	Tested
Endotoxin	≤5 EU/mL	*Not Tested	Tested

Notes: *Safety tests were not performed for manufacturing development.

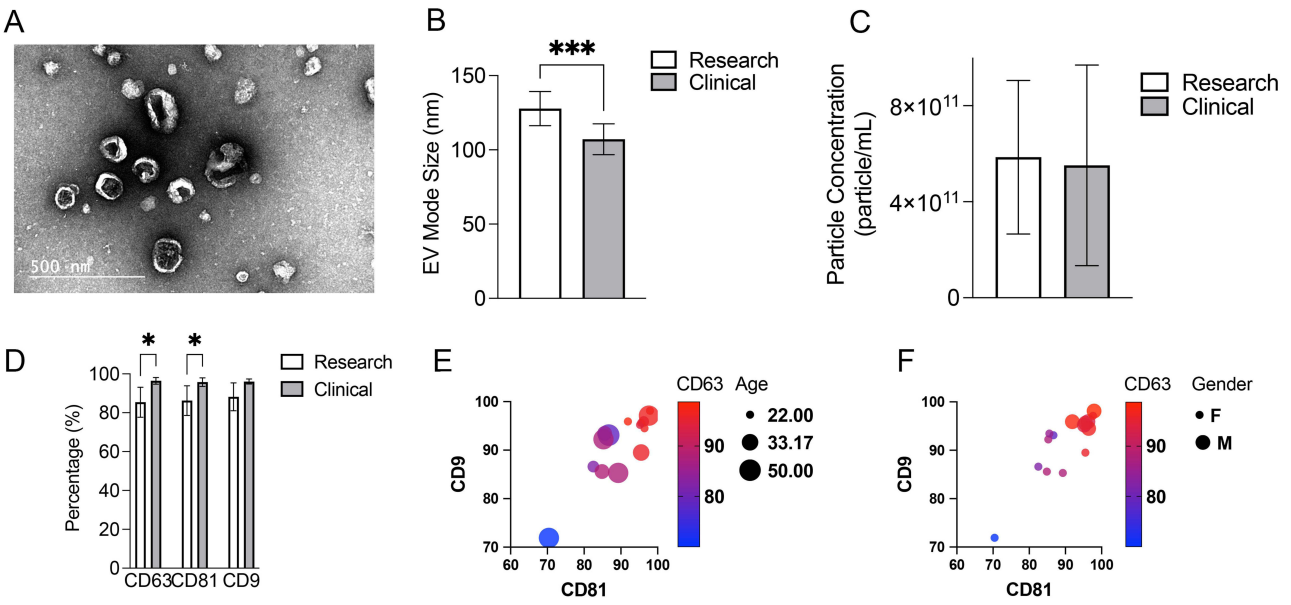

Figure 2 Phenotypical characterization of SCEVs from both research and clinical batches. (**A**) Electron micrographs of SCEVs revealed that the nanovesicles were round and elliptical. (**B**) Significant differences in EV Mode Size between research and clinical batches (***p<0.001). (**C**) Large variation in particle concentration of SCEVs between batches in both research and clinical production. Concentration can be affected by final product volume and donor variation. (**D**) Average expression of phenotypical markers of SCEVs, CD63, CD81, and CD9. Significant differences between research and clinical batches were observed for CD63 and CD81 expression (*p<0.05). One of the SCEVs research batches had lower expression of CD63 and CD81, which lowered the overall average of research batch expression. The rest of the SCEVs in the research batches were clustered with higher expressions. (**E**) No obvious clustering was observed with the age of donors to the phenotypical marker distribution of research batches of SCEVs. (**F**) Clustering of phenotypical marker distribution by gender observed in research batches of SCEVs.

with higher phenotypical expression in CD63, CD81, and CD9 than in SCEVs produced by female donors (Figure 2F). However, the difference in phenotypical expression was not observed in clinical batches where both male and female donors were used. Clinical batches of SCEVs tested negative for mycoplasma and sterility and passed endotoxin-level assessments.

SCEVs Promote Similar Neurite Length Growth as NGF

The morphology of rat embryonic hippocampal neurons was similar among the groups (Figure 3A–D). The neurite length measured for treatment with either 6×10^{9} or 6×10^{10} SCEV particles/mL (research batches of SCEVs only,

Table 2 Characterization and Quality Metrics of Research SCEVs Batches

Sample	Donor Info		Passage/ Batch	Concentration (Particle/mL)	Phenotype (%)			Total Protein (mg/mL)	EVs Mode Size (nm)
	Age	Gender			CD63	CD81	CD9		
HSC366	33	F	P3, batch 1	8.53×10^{11}	95.9	95.5	89.5	0.34	137.1
			P3, batch 2	8.30×10^{10}	–	–	–	0.342	123.2
			P3, batch 3	5.40×10^{11}	–	–	–	0.256	120.9
			P3, batch 4	1.28×10^{12}	–	–	–	0.265	137.5
			P3, batch 5	2.92×10^{11}	–	–	–	0.39	133.3
			P3, batch 6	6.17×10^{11}	–	–	–	0.35	125.4
			P2, batch 1	9.71×10^{11}	–	–	–	0.29	135.6
			P2, batch 2	7.93×10^{11}	–	–	–	0.31	116.6
			P2, batch 3	6.20×10^{11}	–	–	–	0.59	103.4

(*Continued*)

https://doi.org/10.2147/IJN.S500159

Table 2 (Continued).

Sample	Donor Info		Passage/ Batch	Concentration (Particle/mL)	Phenotype (%)			Total Protein (mg/mL)	EVs Mode Size (nm)
	Age	Gender			CD63	CD81	CD9		
HSC217	23	M	P0, batch 1	5.79×10^{11}	–	–	–	0.29	122
			P1, batch 1	1.61×10^{11}	–	–	–	0.32	113.3
			P2, batch 1	6.49×10^{11}	–	–	–	0.191	130.4
			P3, batch 1	4.98×10^{11}	93.0	96.2	95.9	0.23	131
HSC199	24	F	P3, batch 1	4.50×10^{11}	82.4	82.5	86.6	0.242	128.7
HSC303	50	F	P1, batch 1	2.54×10^{11}	78.6	86.7	93.1	0.18	132.7
HSC265	12	M	P1, batch 1	1.34×10^{12}	–	–	–	0.263	145.1
			P3, batch 3	8.22×10^{11}	–	–	–	0.34	109.9
HSC263	45	F	P1, batch 1	5.76×10^{11}	87.8	89.3	85.3	0.653	137.3
			P1, batch 3	2.13×10^{11}	–	–	–	0.648	111.4
			P1, batch 4	4.34×10^{11}	70.0	70.4	71.9	0.27	135.9
			P1, batch 5	4.22×10^{11}	–	–	–	–	119.4
			P1, batch 6	9.34×10^{11}	87.7	85.2	92.2	0.27	137.9
			P2, batch 1	3.81×10^{11}	–	–	–	–	129.7
HSC317	29	F	P3, batch 1	3.99×10^{11}	85.1	85.6	93.4	0.43	149.2
			P3, batch 2	8.70×10^{11}	88.1	84.9	85.6	0.36	136.4

Note: Entries marked with "–" indicate tests that have not been conducted.

Table 3 Characterization and Quality Metrics of Clinical SCEVs Batches

Sample ID, Gender, Age	Passage /Batch	Concentration (Particle/mL)	Phenotype (%)			EVs Mode Size (nm)	Total Protein (mg/mL)	*Endotoxin	Sterility	Mycoplasma
			CD63	CD81	CD9					
W430322000076 Male, 22 years	P3, batch 1	4.18×10^{11}	97.8	91.9	95.9	97.4	0.34	<0.500	No growth	Negative
	P3, batch 2	3.13×10^{11}	96.7	96.4	94.5	97.7	0.33		No growth	
	P3, batch 3	4.39×10^{11}	98.7	97.9	98.1	103.3	0.30		No growth	
	P3, batch 4	3.60×10^{11}	94.1	95.2	95.2	107.4	–	<0.645	No growth	Negative
	P3, batch 5	3.80×10^{11}	94.9	95.5	95.6	125	–		No growth	
W430322000079 Female, 45 years	P4, batch 1	1.40×10^{12}	96.3	97.6	97.1	111.9	0.48	<0.254	No growth	Negative

Note: *For products to be administered intravenously, the endotoxin level should not exceed 5 EU/kg of recipient's body weight.

n=7 donors each) was significantly greater ($p<0.05$) than neurons with no NGF (Figure 3E). Neurite length in neurons treated with 6×10^{10} SCEV particles/mL was significantly ($p<0.05$) longer than when treated with 10 ng/mL of NGF (Figure 3E).

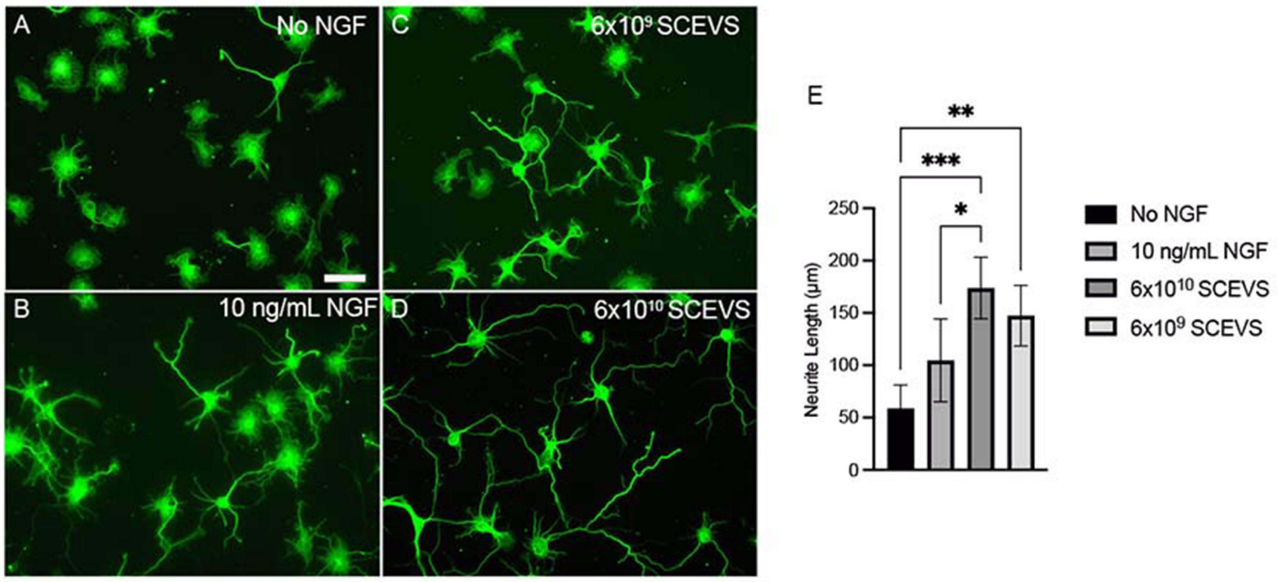

Figure 3 Effects of SCEVs on Neurite Outgrowth. Fluorescent images (**A–D**) of rat hippocampal neurons stained with β-tubulin III. A notable increase in neurite length is observed in neurons treated with 6×10^9 (**C**) or 6×10^{10} (**D**) particles/mL of SCEVs (n=7 donors) compared to the untreated group (**A**) and the group treated with 10 ng/mL of Nerve Growth Factor (NGF) (**B**). Quantitative analysis (**E**) confirms significantly longer neurites in the SCEVs treated group (*p<0.05, **p<0.01, ***p<0.001). Scale bar: 50 µM.

High Correlation of Lipids, Proteins, and miRNA Expression in SCEVs Production

Among three SCEV preparations produced from three different donors, 180 lipids, 2517 proteins, and 732 miRNAs were identified. Lipids and proteins showed very high overlap across all samples, as depicted in the Venn diagram in Figure 4. The miRNA demonstrated less overlap, with about 500 miRNAs shared between at least two samples. Intensity correlations for lipids, proteins, and miRNAs were higher between hSCExo1R and hSCExo2R (research batches), ranging from 0.82 to 1, and lower between the clinical batch hSCExo3C and the two research batches, ranging from 0.69 to 0.96. The lipid expression between hSCExo2R and hSCExo3C showed the lowest correlation.

SCEVs Carried Abundant Triacylglycerol, Diacylglycerol, and Sphingomyelin

To determine the lipid profile of SCEVs, the number of all detected lipid molecules was counted. A total of 180 lipid molecules distributed in 17 lipid subclasses were identified (Figure 5). The lipids subclasses detected were triacylglycerol, phosphatidylcholine, sphingomyelin, phosphatidylethanolamine, diacylglycerol, ceramides, methyl phosphocholine, sphingosine, bis methyl phosphatidic acid, hexosyl-1-ceramide, monoacylglycerol, ceramide phosphoethanolamine, lysophosphatidylcholine, phosphatidylinositol, phosphatidylserine, wax ester, and hexosyl-1-ceramide. From this list, triacylglycerol (54 counts/30%) and phosphatidylcholine (45 counts/25%) are the top 2 in terms of intensity levels, comprising 55% of total lipid in SCEVs, followed by sphingomyelin (25 counts/14%), phosphatidylethanolamine (15 counts/8%), diacylglycerol (10 counts/6%), and ceramides (7 counts/4%). The remaining lipid subclasses represented less than 4% of the total content each.

SCEVs Carried Proteins for Axon Guidance, Growth, Regeneration and Angiogenesis

To determine the protein profile of SCEVs, the 2517 detected proteins were ranked based on intensity levels. To restrict the number of proteins used for functional enrichment analysis, we focused on those most highly expressed, the 1259 proteins above the median. We used the DAVID v2023q4 database of functional annotation tools to generate a table ranked based on the FDR, considering 0.05 as the cutoff. We found 136 terms associated with nervous system regeneration (Supplementary Table 1). The top 3 terms found were axon guidance, followed by other terms related to axon growth, such as NCAM signaling for neurite out-growth, regulation of expression of SLITs and ROBOs, signaling by ROBOs receptors, cell adhesion, actin filament binding, and integrin binding (Table 4). Terms related to signaling

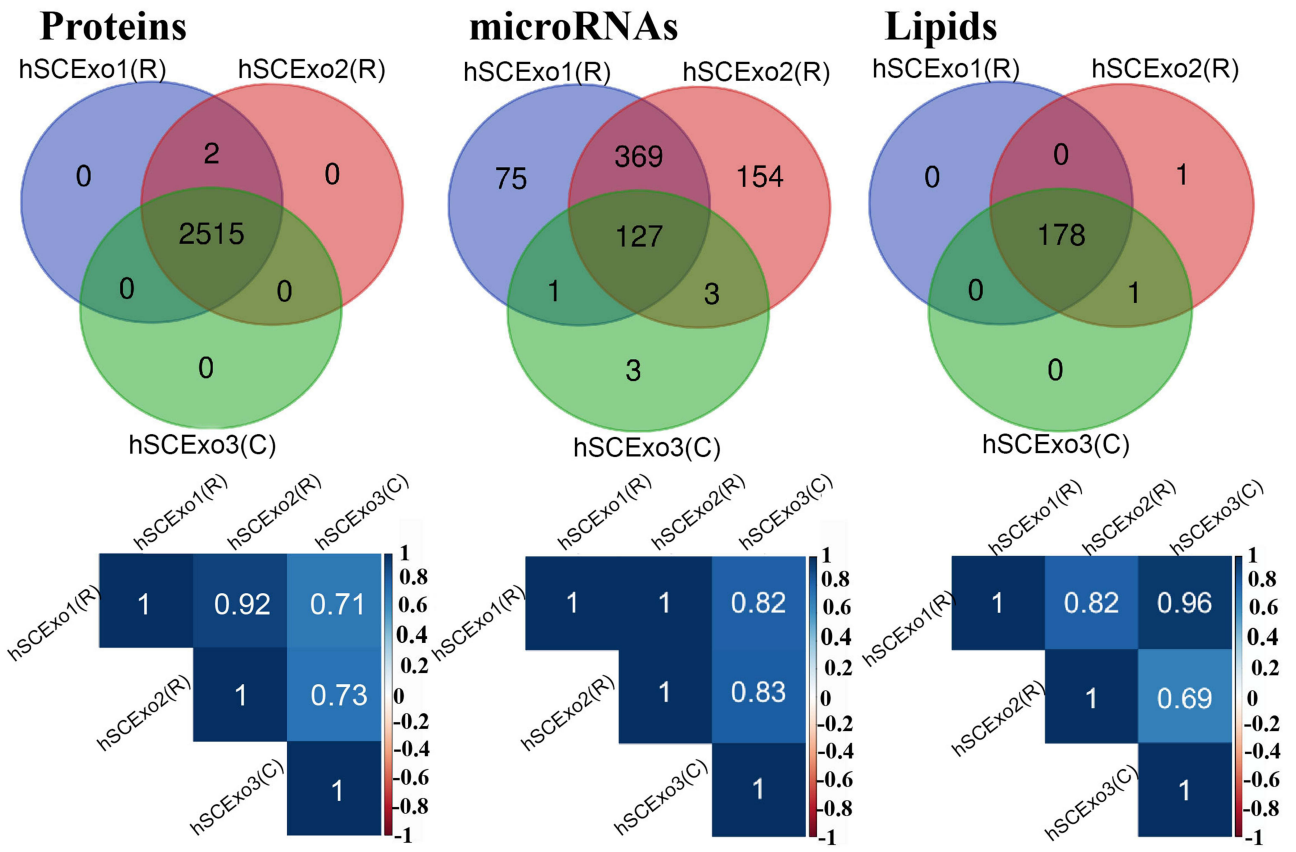

Figure 4 Comparative Analysis of Lipids, Proteins, and miRNAs in SCEVs. This figure illustrates the overlap and correlation in the contents of SCEVs (hSCExo1R, hSCExo2R, hSCExo3C) through Venn diagrams and Pearson correlation coefficient heat maps. The Venn diagrams reveal a substantial overlap in lipids and proteins across the samples, with a moderate overlap for miRNAs. A total of 180 lipids, 2517 proteins, and 732 miRNAs were identified. Meanwhile, the heat maps below each diagram demonstrate high to very high correlations in the intensity levels of these molecules among the three EVs samples, indicating consistency in exosomal content across different preparations.

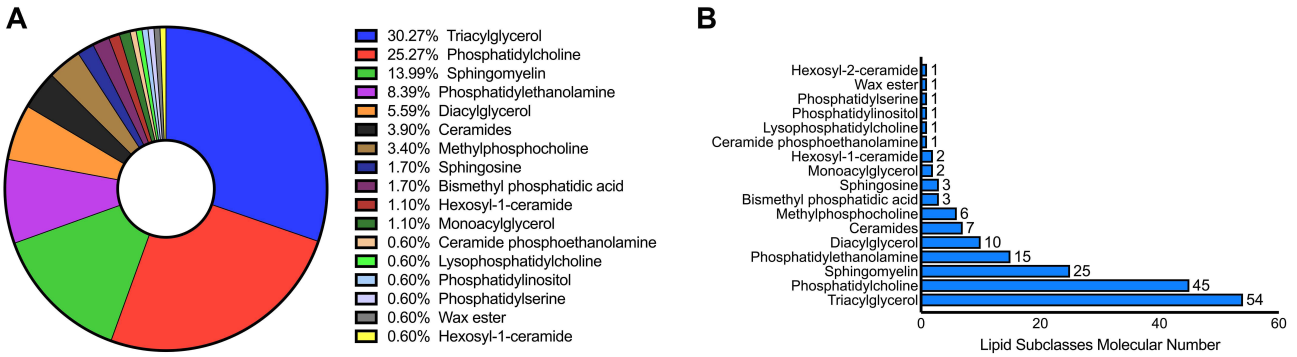

Figure 5 Distribution of Lipid Subclasses in Human SCEVs. The composition and distribution of lipid molecules (total of 180) were within 17 distinct subclasses in SCEVs (**A**) emphasizing the dominance of triacylglycerol and phosphatidylcholine. Triacylglycerol and phosphatidylcholine are the most prevalent, constituting 55% of the total lipid content (**B**).

pathways associated with nervous system regeneration included the VEGFA-VEGFR2 signaling pathway, MAPK family signaling cascades, ROBO receptor signaling, the brain-derived neurotrophic factor signaling pathway, and the phosphatidylinositol 3-kinase-AKT signaling pathway. Cell survival and proliferation terms included negative regulation of apoptotic processes and cellular responses to growth factor stimulus; angiogenesis, including VEGF signaling, was also enriched in SCEVs (Table 4).

Table 4 Key Proteomic Terms of SCEVs Linked to Nervous System (NS) Regeneration

Category	Top 10 terms related to axon growth/extension	FDR < 0.05
GOTERM_MF_DIRECT	- GO:0005515~protein binding	3.02E-40
GOTERM_MF_DIRECT	- GO:0045296~cadherin binding	1.26E-33
REACTOME_PATHWAY	- R-HSA-422475~Axon guidance	1.38E-31
REACTOME_PATHWAY	- R-HSA-9675108~Nervous system development	2.16E-31
REACTOME_PATHWAY	- R-HSA-9010553~Regulation of expression of SLITs and ROBOs	1.62E-29
REACTOME_PATHWAY	- R-HSA-376176~Signaling by ROBO receptors	7.90E-26
REACTOME_PATHWAY	- R-HSA-1474244~Extracellular matrix organization	1.23E-14
GOTERM_BP_DIRECT	- GO:0007155~cell adhesion	7.77E-14
GOTERM_MF_DIRECT	- GO:0005178~integrin binding	1.27E-13
GOTERM_MF_DIRECT	- GO:0051015~actin filament binding	4.29E-13
Top 10 terms related to signaling pathways regulating nervous system regeneration		
REACTOME_PATHWAY	- R-HSA-376176~Signaling by ROBO receptors	7.90E-26
REACTOME_PATHWAY	- R-HSA-9604323~Negative regulation of NOTCH4 signaling	1.34E-12
REACTOME_PATHWAY	- R-HSA-8948751~Regulation of PTEN stability and activity	3.44E-12
REACTOME_PATHWAY	- R-HSA-6807070~PTEN Regulation	2.93E-07
WIKIPATHWAYS	- WP3888: VEGFA VEGFR2 signaling	3.51E-07
REACTOME_PATHWAY	- R-HSA-194315~Signaling by Rho GTPases	1.73E-06
REACTOME_PATHWAY	- R-HSA-5684996~MAPK1/MAPK3 signaling	2.41E-06
REACTOME_PATHWAY	- R-HSA-5683057~MAPK family signaling cascades	1.13E-05
GOTERM_BP_DIRECT	- GO:2001046~positive regulation of integrin-mediated signaling pathway	3.60E-05
REACTOME_PATHWAY	- R-HSA-1257604~PIP3 activates AKT signaling	5.28E-05
Top 10 terms related to VEGF signaling and angiogenesis		
REACTOME_PATHWAY	- R-HSA-1234174~Cellular response to hypoxia	5.19E-09
GOTERM_BP_DIRECT	- GO:0001525~angiogenesis	3.42E-07
WIKIPATHWAYS	- WP3888: VEGFA VEGFR2 signaling	3.51E-07
REACTOME_PATHWAY	- R-HSA-9013026~RHOB GTPase cycle	2.68E-06
REACTOME_PATHWAY	- R-HSA-9013409~RHOJ GTPase cycle	3.77E-04
REACTOME_PATHWAY	- R-HSA-4420097~VEGFA-VEGFR2 Pathway	7.74E-04
REACTOME_PATHWAY	- R-HSA-194138~Signaling by VEGF	0.0025131
KEGG_PATHWAY	- hsa04066:HIF-1 signaling pathway	0.0066651
KEGG_PATHWAY	- hsa04371:Apelin signaling pathway	0.0173103
REACTOME_PATHWAY	- R-HSA-9013408~RHOG GTPase cycle	0.0245688
Terms related to cell survival and proliferation		
REACTOME_PATHWAY	- R-HSA-8948751~Regulation of PTEN stability and activity	3.44E-12
REACTOME_PATHWAY	- R-HSA-6807070~PTEN Regulation	2.93E-07
REACTOME_PATHWAY	- R-HSA-1257604~PIP3 activates AKT signaling	5.28E-05
GOTERM_BP_DIRECT	- GO:0043066~negative regulation of apoptotic process	9.97E-04
KEGG_PATHWAY	- hsa04151: PI3K-Akt signaling pathway	0.007554
GOTERM_BP_DIRECT	- GO:0071363~cellular response to growth factor stimulus	0.0149294
GOTERM_BP_DIRECT	- GO:0042127~regulation of cell proliferation	0.0241039
REACTOME_PATHWAY	- R-HSA-69278~Cell Cycle, Mitotic	0.0271516
GOTERM_BP_DIRECT	- GO:0060548~negative regulation of cell death	0.0426774

miRNA of SCEVs Potentially Target Genes Related to Apoptosis, Inflammation, and Inhibition of Axon Regeneration

miRNA profiles of SCEVs exhibited potential target genes related to apoptosis, inflammatory response, and inhibition of regeneration (Figure 6). For the apoptosis pathway, caspase 3 and caspase 9 are potential targets of hsa-let-7a-5p, hsa-let

-7c-5p, hsa-let-7g-5p, hsa-98-5p, and hsa-155-5p. For inflammatory pathways, IL-2, IL-6, IL-12, IL-6R, IL-1ß, TNF, NFKB are potential targets of hsa-let-7i-5p, hsa-143-3p, hsa-21-5p, hsa-98-5p, hsa-23-3p, and hsa-155-5p. hsa-155-5p can also regulate PTEN, an inhibitor of axon regeneration (Figure 6).

The activity profiles of the top 30 SCEV miRNAs were ranked by expression levels, and their known roles in promoting nervous system regeneration were determined by searching the PubMed database (Table 5). Key signaling pathways found were related to nervous system regeneration, including the PTEN/PI3K/Akt/mTOR pathway, cAMP/PKA pathway, and Wnt/ß-catenin signaling, among others. We also found several miRNAs that influence repair and/or regeneration in different injuries and disease types, such as spinal cord injury, traumatic brain injury, peripheral nerve injury, retinal ganglion cell injury, cerebral ischemia injury, neurodegenerative diseases, diabetic neuropathy, glioblastoma, and intrauterine hypoxia (Supplementary Table 2). In addition, we observed that the regeneration-promoting effects of these miRNAs could occur through several mechanisms, including promoting axon growth and neuroprotection, inducing myelination and angiogenesis, and attenuating neuroinflammation (Supplementary Table 3).

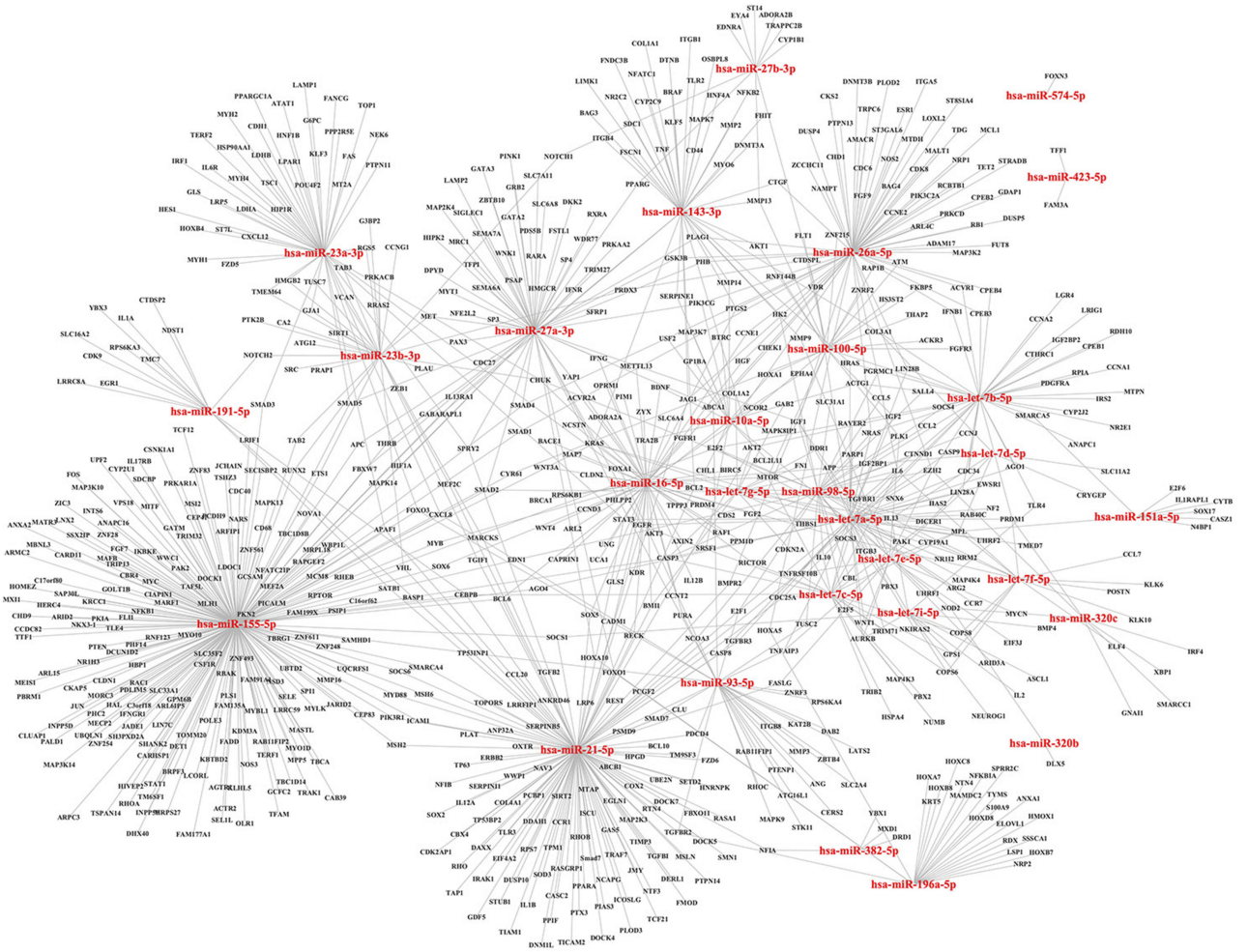

Figure 6 MicroRNA-target gene interaction networks. The interaction network map depicts the top 30 microRNAs and their potential target genes (FDR<0.05). MicroRNAs are illustrated in red as source nodes, and their respective target genes are in black as target nodes. Genes implicated in apoptosis, inflammation, and inhibition of regeneration, including caspase 3, caspase 9, IL-6, IL-1ß, and PTEN, are potential targets of hsa-let-7a-5p, hsa-let-7c-5p, hsa-let-7g-5p, hsa-98-5p, hsa-155-5p, hsa-23a-3p, hsa-21-5p, hsa-155-5p.

Table 5 Functional Roles of Top 30 miRNAs in SCEVs for Nervous System Regeneration

MicroRNA ID	Top 30 miRNAs associated with nervous system regeneration
hsa-let-7a-5p	- Promotes the regrowth of neurons in spinal-cord-injured rats by targeting the HMGA2/SMAD2 axis.[50] - Promotes Krox20 expression and myelination via Notch1 suppression in a mouse model of loss of function.[51] - Enhances neurite growth of mouse dorsal root ganglion neurons after a sciatic nerve crush.[52]
hsa-let-7b-5p	- Reduces cutaneous inflammation thought TLR4/NF-κB/STAT3/AKT signaling pathway and promotes M2 macrophage polarization.[53] - Promotes Krox20 expression and myelination via Notch1 suppression in a mouse model of loss of function.[51]
hsa-let-7i-5p	- Promotes Krox20 expression and myelination via Notch1 suppression in a mouse model of loss of function.[51]
hsa-let-7c-5p	- Attenuates neuroinflammation via promoting microglia M2 polarization and decreases levels of caspase-3 in a murine model of traumatic brain injury.[54] - Promotes Krox20 expression and myelination via Notch1 suppression in a mouse model of loss of function.[51] - Suppresses microglia activation in a mouse model of cerebral ischemia injury.[55]
hsa-let-7f-5p	- Promotes Krox20 expression and myelination via Notch1 suppression in a mouse model of loss of function.[51] - Anti-apoptotic role in Aβ25−35-induced cytotoxicity and improves mesenchymal stem cell survival in Alzheimer disease models.[56] - Enhances neurite growth of mouse dorsal root ganglion neurons after a sciatic nerve crush.[52]
hsa-miR-16-5p	- Mature miRNA related to human axonal regeneration.[57]
hsa-let-7g-5p	- Attenuated Aβ-induced increased permeability and apoptosis of brain microvascular endothelial cells in a human cell line model of Alzheimer's disease in vitro.[58]
hsa-let-7e-5p	- Promotes Krox20 expression and myelination via Notch1 suppression in a mouse model of loss of function.[51] - Inhibits mesenchymal-epithelial transition consistent with the reduction of glioma stem cell phenotypes by targeting VSIG4 in glioblastoma.[59]
hsa-miR-151a-5p	- Its downregulation analyzed in peripheral blood samples of patients with the sporadic form of Amyotrophic lateral sclerosis may impact the phenotypic expression of the disease.
hsa-miR-26a-5p	- Promotes the hippocampal neuronal axon growth by suppressing PTEN and improves retinal ganglion cell survival in mice.[60] - Activates the PTEN-AKT-mTOR pathway to promote axonal regeneration and neurogenesis and attenuates glia scarring in a model of spinal cord injury in rats.[61] - Mature miRNA related to human axonal regeneration.[57]
hsa-miR-320a-3p	- Induces neurite outgrowth of mouse N2a cells by targeting ARPP-1 in vitro.[62]
hsa-miR-423-5p	- Inhibits microglia cells polarization to the M1 phenotype by targeting NLRP3 in a rat model of spinal cord injury.[63] - Promotes angiogenesis via suppressing HIPK2 expression to disinhibit HIF1α/VEGF signaling in vitro model of diabetic neuropathy.[64]
hsa-miR-196a-5p	- Enhances polymerization of neuronal microfilaments through suppressing insulin-like growth factor 2 mRNA binding protein 3 and upregulating IGF2 in in vitro and in vivo mouse models of Huntington's disease.[65] - Enhances neuronal morphology through suppressing RAN binding protein 10 and increasing the ability of β-tubulin polymerization in vitro and in vivo mouse models of Huntington's disease.[66]
hsa-miR-191-5p	- Alleviates microglial cell injury by targeting Map3k12 to inhibit the MAPK signaling pathway in a mouse model of Alzheimer's disease.[67]
hsa-let-7d-5p	- Promotes Krox20 expression and myelination via Notch1 suppression in a mouse model of loss of function.[51]
hsa-miR-100-5p	- Mediates anti-tumorigenic activity in glioblastoma multiforme tumor-initiating cells in vitro.[68]
hsa-miR-143-3p	- Decreases tau phosphorylation, promotes neurite outgrowth and microtubule assembly, attenuates amyloid precursor protein phosphorylation, and reduces the generation of Aβ40 and Aβ42 by targeting Death-associated protein kinase 1 in vitro.[50]
hsa-miR-98-5p	- Attenuates neuronal apoptosis and inflammation after sevoflurane treatment in rats.[69]
hsa-miR-574-5p	- Decreases BACE1 expression and restores synaptic function in the hippocampus and improves spatial memory and learning in a mouse model of PM2.5 exposure.[70]
hsa-miR-10a-5p	- Regulates brain-derived neurotrophic factor in silico.[71] - May be associated with peripheral myelination by targeting Tox4, Xrcc2, and C5ar2.[72]
hsa-miR-320b	- Induces neurite outgrowth of mouse N2a cells by targeting ARPP-1 in vitro.[62]
hsa-miR-23a-3p	- Improves the neurological outcome after traumatic brain injury in mice by inhibiting neurons apoptosis and inflammatory response via reactivating PTEN/AKT/mTOR signaling pathway.[73] - Suppresses oxidative stress and lessened cerebral ischemia-reperfusion injury in a mouse model of focal cerebral ischemia-reperfusion.[74]

(*Continued*)

https://doi.org/10.2147/IJN.S500159

Table 5 (Continued).

MicroRNA ID	Top 30 miRNAs associated with nervous system regeneration
hsa-miR-23b-3p	- Enhances neurite outgrowth by targeting Nrp1 in vitro and improves nerve regeneration in mice.[75] - Protects against Aβ-induced tau hyperphosphorylation by directly targeting GSK-3β and alleviates cognitive deficits by suppressing the GSK-3β/p-tau and Bax/caspase-3 pathways in a mouse model of Alzheimer's disease.[76] - Alleviates the severity of EAE by decreasing microglial inflammation and pyroptosis via the repression of NEK7 in a mouse model of multiple sclerosis.[77] - Suppresses Apaf-1 protein.[78]
hsa-miR-27a-3p	- Reduces neuronal apoptosis and microglia activation in the perihematomal area and reduces brain edema and BBB permeability after intracerebral hemorrhage in rats.[78] - Relieves inflammation, neuronal damage, and neurologic deficit via regulating LITAF and the TLR4/NF-κB pathway in rats with cerebral ischemia reperfusion.[79] - Inhibits the inflammatory response of spinal cord injury by negatively regulating TLR4.[80] - Positively regulates key tight junction proteins, claudin-5 and occludin, at the brain endothelium through targeting GSK3ß gene and activating Wnt/ß-catenin signaling in an in vitro model of the brain endothelium.[81] - Attenuates etoposide-induced changes in Noxa, Puma, and Bax, reduces downstream markers of caspase-dependent (cytochrome c release and caspase activation) and caspase-independent (apoptosis-inducing factor release) pathways, and limited neuronal cell death in an etoposide-induced in vitro model of apoptosis in primary cortical neurons, and attenuated cortical lesion volume and neuronal cell loss in the hippocampus after traumatic brain injury in mice.[82] - Attenuates IR-induced inflammatory damage to the blood-spinal cord barrier by negatively regulating TICAM-2 of the TLR4 signaling pathway and inhibiting the NF-κB/IL-1β pathway in a spinal cord ischemia reperfusion injury model in rats.[83] - Protects dissociated cortical neurons from degeneration in response to peripheral blood mononuclear cell conditioned media in the autoimmune.[84]
hsa-miR-93-5p	- Inhibits retinal neurons apoptosis by inhibiting PDCD4 expression and activating PI3K/Akt pathway in a rat model of acute ocular hypertension.[85] - Inhibits neuropathic pain possibly through inhibiting STAT3-mediated neuroinflammation in a model of rat chronic constriction sciatic nerve injury.[86]
hsa-miR-21-5p	- Promotes neurite growth in rat dorsal root ganglia explant which is associated with PTEN downregulation and PI3-kinase activation in neurons.[87] - Inhibits expression of PTEN and apoptosis and promotes angiogenesis through regulating the expression of apoptosis- and angiogenesis-related molecules in a rat model of traumatic brain injury.[88] - Bounds to PTEN mRNA decreasing its levels and promotes neurite growth after in vivo axotomy in both the adult dorsal root ganglion and embryonic cortical neurons in rats.[89] - Regulates astrocytic function both in vivo and in vitro likely mediated through transforming growth factor beta mediated targeting of the PI3K/AKT/mTOR pathway promoting the functional recovery after spinal cord injury in mice.[90] - Reduces the apoptosis and inflammation through the PI3K/AKT pathway after spinal cord injury in rats.[91]
hsa-miR-320c	- Induces neurite outgrowth of mouse N2a cells by targeting ARPP-1 in vitro.[62]
hsa-miR-155-5p	- Promotes dorsal root ganglion neuron axonal growth via the cAMP/PKA pathway.[92]
hsa-miR-382-5p	- Promotes angiogenesis and activates AKT/mTOR signaling pathway by repressing PTEN in MKN1 human gastric cancer cells both in vitro and in vivo.[93] - Promotes liver regeneration via targeting PTEN-Akt axis both in vitro and in vivo.[122]

Discussion

Based on our reproducible methods to produce clinical grade SCs for clinical trials targeting spinal cord and peripheral nerve injuries,[13–15,18,95] we developed a systematic and reproducible method to generate research and clinical grade human SCEVs. These methods were used to generate SCEVs for treating one ALS patient[11,36] who safely received serial intravenous infusions of allogeneic SCEVs.[11,36] The treatment aimed to investigate the potential for SCEVs to repair the impaired SCs and consequently support motor neuron function. A sural nerve biopsy from the patient confirmed that the cultured SCs appeared senescent, displaying impaired growth capacity, which improved upon exposure to allogeneic SCEVs in vitro. Over a 10-week observation period, the patient's serum neurofilament and cytokine levels did not shown a clear trend, though an in-house assay suggested possible inflammasome activation during the disease course. Importantly, a trend toward clinical stabilization was observed during the infusion period.[11,36] As an alternative to autologous SCEVs, allogeneic SCEVs are off-the-shelf products that could benefit time-sensitive treatments for neurological injuries. Treatment with autologous SCs is less feasible due to the time required for product manufacture and the invasiveness of the surgery for transplantation. Variance in phenotypical markers and particle sizes was observed in the

research SCEV batches, possibly due to batch and donor variability. However, despite the observed variation, SCEVs from various batches and donors were shown to promote neurite extension (Figure 3). This observation suggested that more functional identifiers should be used as part of quality development for SCEVs as therapeutic agents. The molecular profile of human SCEVs generated in this study allowed us to identify and develop functional identifiers in proteomic, lipidomic, and miRNA characteristics that could be used as qualification markers for future clinical products to reduce batch variations and provide the therapeutic potential needed for successful clinical applications. Related indicators to the desired molecular profile can be established as part of donor qualification to reduce donor variability.

This study highlights the variabilities observed in the characteristics of research batches of SCEVs, which may be expected due to the use of different donors due to a combination of genetics, biological, and environmental factors that may not be acknowledged. Donor variability is an inherent challenge in the manufacturing of allogeneic cellular products,[96] as regulations prohibit pooling cellular materials from multiple donors into a single lot. Ideally, extensive large-scale donor characterization involving datasets from dozens to hundreds of donors should be conducted to identify robust trends.[96] However, obtaining such a large number of samples is challenging due to the nature of the source materials. To address these issues and enhance batch consistency, we have implemented several strategies for producing clinical batches of SCEVs and will continue to collect additional data to refine these processes.

Standardized protocols have been adopted across all steps of SCEV production, including cell culture conditions, vesicle isolation techniques, and quality control measures. Comprehensive donor screening processes have been established to identify donors whose cellular products should consistently meet predefined quality parameters, incorporating genetic, metabolic, and health information reviews. Robust quality control systems, including phenotypic and functional testing, should promote consistent biological activity between SCEV batches. Advanced analytical tools, such as flow cytometry, quantitative protein analysis like ELISA and molecular profiling, were utilized to closely monitor and analyze SCEV characteristics, allowing for the early detection of deviations from standard product specifications.

Additionally, batch-to-batch comparisons are conducted to identify sources of variability, leading to adjustments in the manufacturing process to improve product consistency. By continuing to implement these measures and collect molecular profile data for clinical human SCEVs, we aim to ensure that each batch of SCEVs meets regulatory standards and maintains the therapeutic potential required for successful clinical applications.

SC are pivotal in the peripheral nervous system for their role in normal axon function and also to promote axon regeneration and neurite outgrowth.[2] The regenerative capabilities of SCs derive, in part, from their secretion of EVs, which can mediate local and systemic intercellular communication[97,98] through an endocrine-like mechanism.[99] This capacity facilitates communication between cells that are distant from each other, where SCEVs are critical carriers of regenerative signals between them.[87,100,101]

Experimental studies have demonstrated that rat SCEVs enhance recovery following spinal cord injuries, support neurite outgrowth in dorsal root ganglion cultures, and promote axonal regeneration post-axotomy, suggesting their involvement in multiple facets of neuronal repair.[87,101–104] Although human SCs behave differently in some respects from rat SCs in vitro, including senescence and the inability to myelinate axons,[105,106] parallels in the proteomic analysis between rat and human SCEVs further substantiate the hypothesis that they can promote neurite growth across species.[39] Moreover, the high degree of genetic conservation between rodents and humans may support the translational potential of these findings.[107,108]

Herein, we showed that rat hippocampal neurons exposed to human SCEVs exhibited enhanced neurite growth, superior to no treatment and comparable or superior to that induced by 10 ng/mL of nerve growth factor (NGF), a well-known potent neurotrophic factor.[109,110] This bioassay observation underscores the potent bioactive profile of human SCEVs derived from 7 donors capable of supporting neurite growth independent of other external growth factors (Figure 3E). Despite phenotypic variations observed among SCEV research batches derived from different donors, the consistent promotion of neurite outgrowth highlights the intrinsic therapeutic potential of SCEVs. This consistency suggests that the bioactive molecules within SCEVs are robust across variations, making them promising candidates for clinical applications. Given the complexities of translating animal model outcomes to human clinical contexts, incorporating human-derived neuronal models in human SCEV research could enhance these assays' relevance and predictive value. Such models would validate the functionality of SCEVs in a human biological setting and aid in developing

potency assays crucial for clinical product validation. Future investigations should focus on detailed molecular analysis to identify the specific cargo within SCEVs that contribute to their regenerative effects. Understanding these mechanisms will facilitate the development of targeted therapies for neurodegenerative diseases and injury recovery, leveraging the natural regenerative pathways modulated by SCEVs.

We recently reported the effects of SCEVs in a severe TBI rat model.[12,123] Systemic administration of human SCEVs was found to significantly dampen microglial activation and reduce the levels of caspase 1, a marker for inflammasome activation. This suggests an interruption in the secondary inflammatory cascade, often responsible for exacerbating neural damage. Moreover, our analysis revealed a reduction in neural tissue damage and contusion volume, signifying the potential of SCEVs in altering the trajectory of neurotrauma recovery. These findings underscore the promise of SCEVs as a cell-based therapeutic strategy for neurotrauma. By affecting a spectrum of pathological events, from reducing inflammation to fostering repair and regeneration, SCEVs have the potential to enhance neural repair and functional recovery, offering new hope for addressing the multifaceted consequences of TBI.

The proteomic analysis revealed the enrichment of functional networks related to axon growth, cell survival and proliferation, and angiogenesis. Wei et al (2019), using similar culture conditions and EV isolation methods, identified 12 proteins closely related to central nervous system repair in rat SCEV cargo.[39] Several terms from the KEGG pathway and Gene Ontology databases identified in rat SCEVs were concordant with the human SCEVs found in our proteomics, such as axon guidance, regulation of actin cytoskeleton, PI3K-Akt signaling pathway, ECM-receptor interaction, focal adhesion, angiogenesis, negative regulation of apoptotic process, protein binding, and GTP binding. Although rodent and human genomes differ, they share highly conserved genes and networks.[107,108] This may contribute to the similarity in rat and human SCEV cargos and their similar effects on neurite outgrowth in rat hippocampal neurons.

The top 30 expressed miRNAs were analyzed using large databases to determine their potential roles in promoting axon growth and neuroprotection, attenuating neuroinflammation, and inducing myelination and angiogenesis (Table 5). Several of these biological processes are regulated by the PTEN/phosphatidylinositol 3-kinase/AKT/mTOR signaling pathway, which is activated by 4 out of the top 30 miRNAs found in human SCEVs, including miRNA 21–5p.[87,91,111–114] The regulation of PTEN stability and activity is also found to be one of the top signaling pathways in proteomic analysis (Table 4). miRNA related to neuroprotection did not overlap with those related to myelination but mostly overlapped with attenuation of inflammation. While myelination may not be directly involved in early cell survival, myelin regeneration protects preserved neurons and supports functional recovery.[88] Persistent inflammation and neuronal damage are closely related biological processes, and most neurodegenerative diseases are associated with neuroinflammation.[89] The top 30 expressed miRNAs from human SCEVs are involved in key biological processes known to promote nervous system regeneration (Table 5).

The lipidomic analysis has identified a rich composition of lipids in SCEVs, including triacylglycerol, phosphatidylcholine, sphingomyelin, phosphatidylethanolamine, diacylglycerol, and ceramides. There is evidence that lipids are taken up and used by axons to promote axon growth during regeneration[90] and that phospholipids synthesis increases when neurons extend neurites and produce more membranes.[115] Triacylglycerol and diacylglycerol may serve as substrates for the generation of phospholipids during axon regeneration.[115,116] Sphingomyelin is another important constituent of plasma membranes and is enriched in the myelin sheet of some axons. In addition, both sphingomyelin and ceramides have been implicated in axon growth and synaptic plasticity.

The proteomic, miRNA, and lipidomic analysis showed similar overall functional contributions in neural regeneration, but each component has influenced multiple pathways to achieve that purpose. PTEN/phosphatidylinositol 3-kinase/AKT/mTOR in promoting neural regeneration seems to be the common pathway to be influenced by protein and miRNA content. The lipid component supports myelination during axon regeneration, which is not a pathway similar to either the proteomic or the miRNA. The diversity of pathways that the cargo of SCEVs influenced suggested that the molecular mechanisms would be indication-specific and would need to be studied for each intended indication. Therefore, choosing a potency model that best simulates the indication would be essential to explore the molecular mechanism of the therapeutic effects of SCEVs.[117–120]

Study Limitations

The known limitations of miRNA, proteomic, and lipidomic analyses include changes attributable to sample preparation, problems with normalization, and limited sensitivity and specificity.

Conclusion

In conclusion, we have optimized a methodology to obtain large quantities of SCEVs based on clinically validated techniques for human Schwann cells. We characterized the lipid, protein, and miRNA profiles of the human SCEVs, identifying a diverse array of molecules, including those known to have integral roles in nervous system regeneration. Our Pathway analysis findings reveal the therapeutic potential for the molecular cargo of SCEVs, comprising lipids that facilitate membrane dynamics, proteins that guide cellular repair, and miRNAs that regulate key reparative pathways, potentially acting synergistically to support neuroregenerative processes. This comprehensive molecular analysis supports the potential of human SCEVs as a multifaceted therapeutic strategy for treating various neurological conditions, including spinal cord injuries, traumatic brain injuries, and neurodegenerative diseases.

As the field advances, the insights gained from this work are expected to guide the development of EV-based therapy. The study also addresses a significant bottleneck in EV research by providing a scalable and efficient platform for clinical-grade SCEVs production, enabling more extensive studies on EV-mediated communication and repair mechanisms. This, in turn, could support the development of EV-engineering strategies for targeted therapy delivery, further expanding the utility of EVs in medicine.[121,122]

The therapeutic promise of human SCEVs highlighted by our study will require further validation through rigorous in vivo studies using rodent models to replicate and extend these findings in a physiological context. Additionally, exploratory studies utilizing human-induced pluripotent stem cell-derived neurons will inform the translational potential of SCEVs in human cellular environments. These future studies will help confirm the efficacy of SCEVs and refine their therapeutic application, ensuring that human SCEVs can be effectively integrated into clinical strategies for neurological repair and regeneration.

Acknowledgment

We extend our gratitude to Dr. Sam Salama and Dr. Louay Al Hatem from the Life Alliance Organ Recovery Agency (LAORA), University of Miami, FL, for their invaluable assistance in providing an allogeneic healthy donor nerve. We thank Vania Almeida of the Transmission Electron Microscopy Core at the University of Miami for her meticulous work in TEM sample preparation and assistance with the generation of EM images. We thank Creative Biolabs NY, USA, for preparing and processing EV samples for RNA-seq, proteomic, and lipidomic analysis. The work is funded by NIH grant (NIH R37133195, WDD), The Miami Project to Cure Paralysis, the Buoniconti Fund, and the Interdisciplinary Stem Cell Institute.

Funding

The work is funded by NIH grant (NIH R37133195, WDD), Miami Project to Cure Paralysis, the Buoniconti Fund, and the Interdisciplinary Stem Cell Institute. DDP would like to acknowledge support from The John M. and Jocelyn H.K. Watkins Distinguished Chair in Cell Therapies.

Disclosure

The authors have no conflicts related to this paper.

References

1. Illis LS. Central nervous system regeneration does not occur. *Spinal Cord*. 2012;50:259–263. [PMID: 22105462]. doi:10.1038/sc.2011.132
2. Oliveira JT, Yanick C, Wein N, Gomez Limia CE. Neuron-Schwann cell interactions in peripheral nervous system homeostasis, disease, and preclinical treatment. *Front Cell Neurosci*. 2023;17:1248922. [PMID: 37900588]. doi:10.3389/fncel.2023.1248922
3. Gomez-Sanchez JA, Carty L, Iruarrizaga-Lejarreta M, et al. Schwann cell autophagy, myelinophagy, initiates myelin clearance from injured nerves. *J Cell Biol*. 2015;210:153–168. [PMID: 26150392]. doi:10.1083/jcb.201503019
4. Takenaka T, Ohnishi Y, Yamamoto M, Setoyama D, Kishima H. Glycolytic system in axons supplement decreased ATP levels after axotomy of the peripheral nerve. *eNeuro*. 2023:ENEURO.0353–22.2023. PMID: 36894321. doi:10.1523/ENEURO.0353-22.2023

5. Mietto BS, Jhelum P, Schulz K, David S. Schwann cells provide iron to axonal mitochondria and its role in nerve regeneration. *J Neurosci*. 2021;41:7300–7313. [PMID: 34272312]. doi:10.1523/JNEUROSCI.0900-21.2021
6. Court FA, Hendriks WT, MacGillavry HD, Alvarez J, van Minnen J. Schwann cell to axon transfer of ribosomes: toward a novel understanding of the role of glia in the nervous system. *J Neurosci*. 2008;28:11024–11029. [PMID: 18945910]. doi:10.1523/JNEUROSCI.2429-08.2008
7. Hoke A, Redett R, Hameed H, et al. Schwann cells express motor and sensory phenotypes that regulate axon regeneration. *J Neurosci*. 2006;26:9646–9655. [PMID: 16988035]. doi:10.1523/JNEUROSCI.1620-06.2006
8. Sahenk Z, Oblinger J, Edwards C. Neurotrophin-3 deficient Schwann cells impair nerve regeneration. *Exp Neurol*. 2008;212:552–556. [PMID: 18511043]. doi:10.1016/j.expneurol.2008.04.015
9. McGarvey ML, Baron-Van Evercooren A, Kleinman HK, Dubois-Dalcq M. Synthesis and effects of basement membrane components in cultured rat Schwann cells. *Dev Biol*. 1984;105:18–28. [PMID: 6381174]. doi:10.1016/0012-1606(84)90257-4
10. Stoll G, Jander S, Myers RR. Degeneration and regeneration of the peripheral nervous system: from Augustus Waller's observations to neuroinflammation. *J Peripher Nerv Syst*. 2002;7:13–27. [PMID: 11939348]. doi:10.1046/j.1529-8027.2002.02002.x
11. Goldschmidt-Clermont PJ, Khan A, Guest JD, et al. A novel therapy for ALS: allogeneic schwann cell extracellular vesicles. *medRxiv*. 2023;2023:1PMID.
12. Nishimura K, Sanchez-Molano J, Kerr N, et al. Beneficial effects of human Schwann cell-derived exosomes in mitigating secondary damage after penetrating ballistic-like brain injury. *J Neurotrauma*. 2024;41:2395–2412. [PMID: 38445369]. doi:10.1089/neu.2023.0650
13. Anderson KD, Guest JD, Dietrich WD, et al. Safety of autologous human schwann cell transplantation in subacute thoracic spinal cord injury. *J Neurotrauma*. 2017;34:2950–2963. [PMID: 28225648]. doi:10.1089/neu.2016.4895
14. Gant KL, Guest JD, Palermo AE, et al. Phase 1 safety trial of autologous human schwann cell transplantation in chronic spinal cord injury. *J Neurotrauma*. 2022;39:285–299. [PMID: 33757304]. doi:10.1089/neu.2020.7590
15. Gersey ZC, Burks SS, Anderson KD, et al. First human experience with autologous Schwann cells to supplement sciatic nerve repair: report of 2 cases with long-term follow-up. *Neurosurg Focus*. 2017;42:E2. [PMID: 28245668]. doi:10.3171/2016.12.FOCUS16474
16. Khan A, Bellio MA, Schulman IH, et al. The interdisciplinary stem cell institute's use of food and drug administration-expanded access guidelines to provide experimental cell therapy to patients with rare serious diseases. *Front Cell Dev Biol*. 2021;9:675738. [PMID: 34169074]. doi:10.3389/fcell.2021.675738
17. Khan A, Diaz A, Brooks AE, et al. Scalable culture techniques to generate large numbers of purified human Schwann cells for clinical trials in human spinal cord and peripheral nerve injuries. *J Neurosurg Spine*. 2022;36:135–144. [PMID: 34479193]. doi:10.3171/2020.11.SPINE201433
18. Levi AD, Burks SS, Anderson KD, Dididze M, Khan A, Dietrich WD. The use of autologous Schwann cells to supplement sciatic nerve repair with a large gap: first in human experience. *Cell Transplant*. 2016;25:1395–1403. [PMID: 26610173]. doi:10.3727/096368915X690198
19. Santamaria AJ, Benavides FD, Saraiva PM, et al. Neurophysiological Changes in the First Year After Cell Transplantation in Sub-acute Complete Paraplegia. *Front Neurol*. 2020;11:514181. [PMID: 33536992]. doi:10.3389/fneur.2020.514181
20. Monje PV, Deng L, Xu XM. Human Schwann cell transplantation for spinal cord injury: prospects and challenges in translational medicine. *Front Cell Neurosci*. 2021;15:690894. [PMID: 34220455]. doi:10.3389/fncel.2021.690894
21. Ghosh M, Pearse DD. Schwann Cell-Derived Exosomal Vesicles: a Promising Therapy for the Injured Spinal Cord. *Int J mol Sci*. 2023;24:17317. [PMID: 38139147]. doi:10.3390/ijms242417317
22. Isola AL, Chen S. Exosomes: the Messengers of Health and Disease. *Curr Neuropharmacol*. 2017;15:157–165. [PMID: 27568544]. doi:10.2174/1570159X14666160825160421
23. Al-Ali H, Blackmore M, Bixby JL, Lemmon VP. High Content Screening with Primary Neurons. In: Markossian S, Grossman A, Arkin M, et al., editors.*Assay Guidance Manual*.Bethesda (MD);2004.
24. Yang DP, Zhang DP, Mak KS, Bonder DE, Pomeroy SL, Kim HA. Schwann cell proliferation during Wallerian degeneration is not necessary for regeneration and remyelination of the peripheral nerves: axon-dependent removal of newly generated Schwann cells by apoptosis. *mol Cell Neurosci*. 2008;38:80–88. [PMID: 18374600]. doi:10.1016/j.mcn.2008.01.017
25. Leung DW, Cachianes G, Kuang WJ, Goeddel DV, Ferrara N. Vascular endothelial growth factor is a secreted angiogenic mitogen. *Science*. 1989;246:1306–1309. [PMID: 2479986]. doi:10.1126/science.2479986
26. Ruiz de Almodovar C, Fabre PJ, Knevels E, et al. VEGF mediates commissural axon chemoattraction through its receptor Flk1. *Neuron*. 2011;70:966–978. [PMID: 21658588]. doi:10.1016/j.neuron.2011.04.014
27. Ruiz de Almodovar C, Coulon C, Salin PA, et al. Matrix-binding vascular endothelial growth factor (VEGF) isoforms guide granule cell migration in the cerebellum via VEGF receptor Flk1. *J Neurosci*. 2010;30:15052–15066. [PMID: 21068311]. doi:10.1523/JNEUROSCI.0477-10.2010
28. Hattori Y, Shimada T, Yasui T, Kaji N, Baba Y. Micro- and nanopillar chips for continuous separation of extracellular vesicles. *Anal Chem*. 2019;91:6514–6521. [PMID: 31035752]. doi:10.1021/acs.analchem.8b05538
29. Lebreton B, Brown A, van Reis R. Application of high-performance tangential flow filtration (HPTFF) to the purification of a human pharmaceutical antibody fragment expressed in Escherichia coli. *Biotechnol Bioeng*. 2008;100:964–974. [PMID: 18393314]. doi:10.1002/bit.21842
30. Li P, Kaslan M, Lee SH, Yao J, Gao Z. Progress in exosome isolation techniques. *Theranostics*. 2017;7(3):789–804. [PMID: 28255367]. doi:10.7150/thno.18133
31. Livshits MA, Khomyakova E, Evtushenko EG, et al. Isolation of exosomes by differential centrifugation: theoretical analysis of a commonly used protocol. *Sci Rep*. 2015;5:17319. [PMID: 26616523]. doi:10.1038/srep17319
32. Luo X, An M, Cuneo KC, Lubman DM, Li L. High-performance chemical isotope labeling liquid chromatography mass spectrometry for exosome metabolomics. *Anal Chem*. 2018;90:8314–8319. [PMID: 29920066]. doi:10.1021/acs.analchem.8b01726
33. Shirejini SZ, Inci F. The Yin and Yang of exosome isolation methods: conventional practice, microfluidics, and commercial kits. *Biotechnol Adv*. 2022;54:107814. [PMID: 34389465]. doi:10.1016/j.biotechadv.2021.107814
34. Reed SL, Escayg A. Extracellular vesicles in the treatment of neurological disorders. *Neurobiol Dis*. 2021;157:105445. [PMID: 34271084]. doi:10.1016/j.nbd.2021.105445
35. Zhu S, Chen L, Wang M, et al. Schwann cell-derived extracellular vesicles as a potential therapy for retinal ganglion cell degeneration. *J Control Release*. 2023;363:641–656. [PMID: 37820984]. doi:10.1016/j.jconrel.2023.10.012

36. Goldschmidt-Clermont PJ, Khan A, Jimsheleishvili G, et al. Treating amyotrophic lateral sclerosis with allogeneic Schwann cell-derived exosomal vesicles: a case report. *Neural Regen Res*. 2025;20:1207–1216. [PMID: 38922880]. doi:10.4103/NRR.NRR-D-23-01815
37. Huang JH, Chen YN, He H, Fu CH, Xu ZY, Lin FY. Schwann cells-derived exosomes promote functional recovery after spinal cord injury by promoting angiogenesis. *Front Cell Neurosci*. 2022;16:1077071. [PMID: 36687521]. doi:10.3389/fncel.2022.1077071
38. Pan D, Li Y, Yang F, et al. Increasing toll-like receptor 2 on astrocytes induced by Schwann cell-derived exosomes promotes recovery by inhibiting CSPGs deposition after spinal cord injury. *J Neuroinflammation*. 2021;18:172. [PMID: 34372877]. doi:10.1186/s12974-021-02215-x
39. Wei Z, Fan B, Ding H, et al. Proteomics analysis of Schwann cell-derived exosomes: a novel therapeutic strategy for central nervous system injury. *mol Cell Biochem*. 2019;457:51–59. [PMID: 30830528]. doi:10.1007/s11010-019-03511-0
40. Maggio S, Ceccaroli P, Polidori E, Cioccoloni A, Stocchi V, Guescini M. Signal exchange through extracellular vesicles in neuromuscular junction establishment and maintenance: from physiology to Pathology. *Int J mol Sci*. 2019;20:2804. [PMID: 31181747]. doi:10.3390/ijms20112804
41. S U. Food drug administration. human cells, tissues, and cellular and tissue-based product, 21 C.F.R. 2023.
42. PSB Ugent. Venn Diagram Generator. 2023.
43. Licursi V, Conte F, Fiscon G, Paci P. MIENTURNET: an interactive web tool for microRNA-target enrichment and network-based analysis. *BMC Bioinform*. 2019;20(1):545. [PMID: 31684860]. doi:10.1186/s12859-019-3105-x
44. Huang HY, Lin YC, Cui S, et al. miRTarBase update 2022: an informative resource for experimentally validated miRNA-target interactions. *Nucleic Acids Res*. 2022;50:D222–D230. [PMID: 34850920]. doi:10.1093/nar/gkab1079
45. National Cancer Institute. *DAVID: Database for Annotation, Visualization, and Integrated Discovery*; 2024.
46. RapidTables. Pie Chart Maker. 2024.
47. U. S. Food Drug Administration. Sterility. 2023. 21 C.F.R. § 610.12 (2023c).
48. U. S. Food Drug Administration. Food Drug Administration. Guidance for FDA reviewers and sponsors: content and review of chemistry, manufacturing, and control (CMC) information for human somatic cell therapy investigational new drug applications (INDs). *Journal of Human Reproductive Sciences*. 2008;1:19–24. doi:10.4103/0974-1208.39592
49. U. S. Food Drug Administration. Bacterial Endotoxins/Pyrogens. 2014.
50. Wang L, Shui X, Mei Y, et al. miR-143-3p inhibits aberrant tau phosphorylation and amyloidogenic processing of app by directly targeting DAPK1 in Alzheimer's disease. *Int J mol Sci*. 2022;23:7992. [PMID: 35887339]. doi:10.3390/ijms23147992
51. Gökbuget D, Pereira JA, Bachofner S, et al. The Lin28/let-7 axis is critical for myelination in the peripheral nervous system. *Nat Commun*. 2015;6:8584. [PMID: 26466203]. doi:10.1038/ncomms9584
52. Motti D, Lerch JK, Danzi MC, et al. Identification of miRNAs involved in DRG neurite outgrowth and their putative targets. *FEBS Lett*. 2017;591:2091–2105. [PMID: 28626869]. doi:10.1002/1873-3468.12718
53. Xia T, Zhang M, Lei W, et al. Advances in the role of STAT3 in macrophage polarization. *Front Immunol*. 2023;14:1160719. [PMID: 37081874]. doi:10.3389/fimmu.2023.1160719
54. Lv J, Zeng Y, Qian Y, Dong J, Zhang Z, Zhang J. MicroRNA let-7c-5p improves neurological outcomes in a murine model of traumatic brain injury by suppressing neuroinflammation and regulating microglial activation. *Brain Res*. 2018;1685:91–104. [PMID: 29408500]. doi:10.1016/j.brainres.2018.01.032
55. Ni J, Wang X, Chen S, et al. MicroRNA let-7c-5p protects against cerebral ischemia injury via mechanisms involving the inhibition of microglia activation. *Brain Behav Immun*. 2015;49:75–85. [PMID: 25934573]. doi:10.1016/j.bbi.2015.04.014
56. Han L, Zhou Y, Zhang R, et al. MicroRNA Let-7f-5p promotes bone marrow mesenchymal stem cells survival by targeting Caspase-3 in Alzheimer disease model. *Front Neurosci*. 2018;12:333. [PMID: 29872375]. doi:10.3389/fnins.2018.00333
57. Su LN, Song XQ, Xue ZX, Zheng CQ, Yin HF, Wei HP. Network analysis of microRNAs, transcription factors, and target genes involved in axon regeneration. *J Zhejiang Univ Sci B*. 2018;19:293–304. [PMID: 29616505]. doi:10.1631/jzus.B1700179
58. Wu M, Gao Y, Chen B. Mechanism of acteoside-activated let-7g-5P attenuating Abeta-induced increased permeability and apoptosis of brain microvascular endothelial cells based on experimental and network pharmacology. *NeuroReport*. 2022;33:714–722. [PMID: 36165002]. doi:10.1097/WNR.0000000000001837
59. Zhang XH, Qian Y, Li Z, Zhang NN, Xie YJ. Let-7g-5p inhibits epithelial-mesenchymal transition consistent with reduction of glioma stem cell phenotypes by targeting VSIG4 in glioblastoma. *Oncol Rep*. 2016;36:2967–2975. [PMID: 27634309]. doi:10.3892/or.2016.5098
60. Zhang J, Ma Y-X, Zeng Y-Q, et al. miR-26a promotes axon regeneration in the mammalian central nervous system by suppressing PTEN expression. *Acta Biochim Biophys Sin*. 2021;53:758–765.
61. Chen Y, Tian Z, He L, et al. Exosomes derived from miR-26a-modified MSCs promote axonal regeneration via the PTEN/AKT/mTOR pathway following spinal cord injury. *Stem Cell Res Ther*. 2021;12:224. [PMID: 33820561]. doi:10.1186/s13287-021-02282-0
62. White RE, Giffard RG. MicroRNA-320 induces neurite outgrowth by targeting ARPP-19. *NeuroReport*. 2012;23:590–595. [PMID: 22617447]. doi:10.1097/WNR.0b013e3283540394
63. Cheng J, Hao J, Jiang X, et al. Ameliorative effects of miR-423-5p against polarization of microglial cells of the M1 phenotype by targeting a NLRP3 inflammasome signaling pathway. *Int Immunopharmacol*. 2021;99:108006. [PMID: 34339965]. doi:10.1016/j.intimp.2021.108006
64. Xiao Q, Zhao Y, Sun H, Xu J, Li W, Gao L. MiR-423-5p activated by E2F1 promotes neovascularization in diabetic retinopathy by targeting HIPK2. *Diabetol Metab Syndr*. 2021;13:152. [PMID: 34963484]. doi:10.1186/s13098-021-00769-7
65. Yang HI, Huang PY, Chan SC, et al. miR-196a enhances polymerization of neuronal microfilaments through suppressing IMP3 and upregulating IGF2 in Huntington's disease. *mol Ther Nucleic Acids*. 2022;30:286–299. [PMID: 36320323]. doi:10.1016/j.omtn.2022.10.002
66. Her LS, Mao SH, Chang CY, et al. miR-196a enhances neuronal morphology through suppressing RANBP10 to provide neuroprotection in huntington's disease. *Theranostics*. 2017;7:2452–2462. [PMID: 28744327]. doi:10.7150/thno.18813
67. Wan W, Liu G, Li X, et al. MiR-191-5p alleviates microglial cell injury by targeting Map3k12 (mitogen-activated protein kinase kinase kinase 12) to inhibit the MAPK (mitogen-activated protein kinase) signaling pathway in Alzheimer's disease. *Bioengineered*. 2021;12:12678–12690. [PMID: 34818971]. doi:10.1080/21655979.2021.2008638
68. Alrfaei BM, Clark P, Vemuganti R, Kuo JS. MicroRNA miR-100 decreases glioblastoma growth by targeting SMARCA5 and ErbB3 in tumor-initiating cells. *Technol Cancer Res Treat*. 2020;19:1533033820960748. [PMID: 32945237]. doi:10.1177/1533033820960748

69. Zhao L, Wang Z, Chen H, et al. Effects of lncRNA HOXA11-AS on Sevoflurane-induced neuronal apoptosis and inflammatory responses by regulating miR-98-5p/EphA4. *Mediators Inflamm*. 2023;2023:7750134. [PMID: 37064501]. doi:10.1155/2023/7750134
70. Ku T, Li B, Gao R, et al. NF-kappaB-regulated microRNA-574-5p underlies synaptic and cognitive impairment in response to atmospheric PM (2.5) aspiration. *Part Fibre Toxicol*. 2017;14:34. [PMID: 28851397]. doi:10.1186/s12989-017-0215-3
71. Müller S. In silico analysis of regulatory networks underlines the role of miR-10b-5p and its target BDNF in huntington's disease. *Transl Neurodegener*. 2014;3:17. [PMID: 25210621]. doi:10.1186/2047-9158-3-17
72. Wu X. Genome expression profiling predicts the molecular mechanism of peripheral myelination. *Int J Mol Med*. 2018;41:1500–1508. [PMID: 29286075]. doi:10.3892/ijmm.2017.3348
73. Li Z, Xu R, Zhu X, Li Y, Wang Y, Xu W. MicroRNA-23a-3p improves traumatic brain injury through modulating the neurological apoptosis and inflammation response in mice. *Cell Cycle*. 2020;19:24–38. [PMID: 31818176]. doi:10.1080/15384101.2019.1691763
74. Zhao H, Tao Z, Wang R, et al. MicroRNA-23a-3p attenuates oxidative stress injury in a mouse model of focal cerebral ischemia-reperfusion. *Brain Res*. 2014;1592:65–72. [PMID: 25280466]. doi:10.1016/j.brainres.2014.09.055
75. Xia B, Gao J, Li S, et al. Mechanical stimulation of Schwann cells promote peripheral nerve regeneration via extracellular vesicle-mediated transfer of microRNA 23b-3p. *Theranostics*. 2020;10:8974–8995. [PMID: 32802175]. doi:10.7150/thno.44912
76. Jiang H, Liu J, Guo S, et al. miR-23b-3p rescues cognition in Alzheimer's disease by reducing tau phosphorylation and apoptosis via GSK-3beta signaling pathways. *mol Ther Nucleic Acids*. 2022;28:539–557. [PMID: 35592504]. doi:10.1016/j.omtn.2022.04.008
77. Wang J, Sun H, Guo R, et al. Exosomal miR-23b-3p from bone mesenchymal stem cells alleviates experimental autoimmune encephalomyelitis by inhibiting microglial pyroptosis. *Exp Neurol*. 2023;363:114374. [PMID: 36907352]. doi:10.1016/j.expneurol.2023.114374
78. Xi T, Jin F, Zhu Y, et al. miR-27a-3p protects against blood-brain barrier disruption and brain injury after intracerebral hemorrhage by targeting endothelial aquaporin-11. *J Biol Chem*. 2018;293:20041–20050. [PMID: 30337368]. doi:10.1074/jbc.RA118.001858
79. Luo J, Li J, Xiong L, et al. MicroRNA-27a-3p relieves inflammation and neurologic impairment after cerebral ischaemia reperfusion via inhibiting lipopolysaccharide induced TNF factor and the TLR4/NF-kappaB pathway. *Eur J Neurosci*. 2022;56:4013–4030. [PMID: 35584745]. doi:10.1111/ejn.15720
80. Zhang P, Li LQ, Zhang D, Shen Y. Over-expressed miR-27a-3p inhibits inflammatory response to spinal cord injury by decreasing TLR4. *Eur Rev Med Pharmacol Sci*. 2018;22:5416–5423. [PMID: 30229811]. doi:10.26355/eurrev_201809_15800
81. Harati R, Hammad S, Tlili A, Mahfood M, Mabondzo A, Hamoudi R. miR-27a-3p regulates expression of intercellular junctions at the brain endothelium and controls the endothelial barrier permeability. *PLoS One*. 2022;17:e0262152. [PMID: 35025943]. doi:10.1371/journal.pone.0262152
82. Sabirzhanov B, Zhao Z, Stoica BA, et al. Downregulation of miR-23a and miR-27a following experimental traumatic brain injury induces neuronal cell death through activation of proapoptotic Bcl-2 proteins. *J Neurosci*. 2014;34:10055–10071. [PMID: 25057207]. doi:10.1523/JNEUROSCI.1260-14.2014
83. Li XQ, Lv HW, Wang ZL, Tan WF, Fang B, Ma H. MiR-27a ameliorates inflammatory damage to the blood-spinal cord barrier after spinal cord ischemia: reperfusion injury in rats by downregulating TICAM-2 of the TLR4 signaling pathway. *J Neuroinflammation*. 2015;12:25. [PMID: 25876455]. doi:10.1186/s12974-015-0246-3
84. Morquette B, Juzwik CA, Drake SS, et al. MicroRNA-223 protects neurons from degeneration in experimental autoimmune encephalomyelitis. *Brain*. 2019;142:2979–2995. [PMID: 31412103]. doi:10.1093/brain/awz245
85. Tan C, Shi W, Zhang Y, et al. MiR-93-5p inhibits retinal neurons apoptosis by regulating PDCD4 in acute ocular hypertension model. *Life Sci Alliance*. 2023;6:e202201732. [PMID: 37308277]. doi:10.26508/lsa.202201732
86. Yan XT, Ji LJ, Wang Z, et al. MicroRNA-93 alleviates neuropathic pain through targeting signal transducer and activator of transcription 3. *Int Immunopharmacol*. 2017;46:156–162. [PMID: 28284149]. doi:10.1016/j.intimp.2017.01.027
87. Lopez-Leal R, Diaz-Viraque F, Catalan RJ, et al. Schwann cell reprogramming into repair cells increases miRNA-21 expression in exosomes promoting axonal growth. *J Cell Sci*. 2020;133:jcs239004. [PMID: 32409566]. doi:10.1242/jcs.239004
88. Cheng YJ, Wang F, Feng J, et al. Prolonged myelin deficits contribute to neuron loss and functional impairments after ischaemic stroke. *Brain*. 2024;147:1294–1311. [PMID: 38289861]. doi:10.1093/brain/awae029
89. Aktas O, Ullrich O, Infante-Duarte C, Nitsch R, Zipp F. Neuronal damage in brain inflammation. *Arch Neurol*. 2007;64:185–189. [PMID: 17296833]. doi:10.1001/archneur.64.2.185
90. de Chaves EI, Rusinol AE, Vance DE, Campenot RB, Vance JE. Role of lipoproteins in the delivery of lipids to axons during axonal regeneration. *J Biol Chem*. 1997;272:30766–30773. [PMID: 9388216]. doi:10.1074/jbc.272.49.30766
91. Lv X, Liang J, Wang Z. MiR-21-5p reduces apoptosis and inflammation in rats with spinal cord injury through PI3K/AKT pathway. *Panminerva Med*. 2024;66:256–265. [PMID: 32720795]. doi:10.23736/S0031-0808.20.03974-9
92. Wang T, Li B, Wang Z, et al. miR-155-5p promotes dorsal root ganglion neuron axonal growth in an inhibitory microenvironment via the cAMP/PKA pathway. *Int J Biol Sci*. 2019;15:1557–1570. [PMID: 31337984]. doi:10.7150/ijbs.31904
93. Seok JK, Lee SH, Kim MJ, Lee YM. MicroRNA-382 induced by HIF-1alpha is an angiogenic miR targeting the tumor suppressor phosphatase and tensin homolog. *Nucleic Acids Res*. 2014;42:8062–8072. [PMID: 24914051]. doi:10.1093/nar/gku515
94. Bei Y, Song Y, Wang F, et al. miR-382 targeting PTEN-Akt axis promotes liver regeneration. *Oncotarget*. 2016;7:1584–1597. [PMID: 26636539]. doi:10.18632/oncotarget.6444
95. Bellio MA, Khan A. Improving cell production techniques to enhance autologous cell therapy. *Circ Res*. 2018;122:191–193. [PMID: 29348243]. doi:10.1161/CIRCRESAHA.117.312393
96. Silverman LI, Flanagan F, Rodriguez-Granrose D, Simpson K, Saxon LH, Foley KT. Identifying and managing sources of variability in cell therapy manufacturing and clinical trials. *Regen Eng Transl Med*. 2019;5:354–361. doi:10.1007/s40883-019-00129-y
97. Hong P, Yang H, Wu Y, Li K, Tang Z. The functions and clinical application potential of exosomes derived from adipose mesenchymal stem cells: a comprehensive review. *Stem Cell Res Ther*. 2019;10:242. [PMID: 31391108]. doi:10.1186/s13287-019-1358-y
98. Ohayon L, Zhang X, Dutta P. The role of extracellular vesicles in regulating local and systemic inflammation in cardiovascular disease. *Pharmacol Res*. 2021;170:105692. [PMID: 34182130]. doi:10.1016/j.phrs.2021.105692
99. Tetta C, Ghigo E, Silengo L, Deregibus MC, Camussi G. Extracellular vesicles as an emerging mechanism of cell-to-cell communication. *Endocrine*. 2013;44:11–19. [PMID: 23203002]. doi:10.1007/s12020-012-9839-0

100. Hyung S, Kim JY, Jong Yu C, Jung HS, Hong JW. Neuroprotective effect of glial cell-derived exosomes on neurons. *Immunother*. 2019;5:156. PMID: 35813501 doi:10.3389/fncel.2022.920686.
101. Ren J, Zhu B, Gu G, et al. Schwann cell-derived exosomes containing MFG-E8 modify macrophage/microglial polarization for attenuating inflammation via the SOCS3/STAT3 pathway after spinal cord injury. *Cell Death Dis*. 2023;14:70. [PMID: 36717543]. doi:10.1038/s41419-023-05607-4
102. Ching RC, Wiberg M, Kingham PJ. Schwann cell-like differentiated adipose stem cells promote neurite outgrowth via secreted exosomes and RNA transfer. *Stem Cell Res Ther*. 2018;9:266. [PMID: 30309388]. doi:10.1186/s13287-018-1017-8
103. Lopez-Verrilli MA, Picou F, Court FA. Schwann cell-derived exosomes enhance axonal regeneration in the peripheral nervous system. *Glia*. 2013;61:1795–1806. [PMID: 24038411]. doi:10.1002/glia.22558
104. Pan D, Zhu S, Zhang W, et al. Autophagy induced by Schwann cell-derived exosomes promotes recovery after spinal cord injury in rats. *Biotechnol Lett*. 2022;44:129–142. [PMID: 34738222]. doi:10.1007/s10529-021-03198-8
105. Tao Y. Isolation and culture of Schwann cells. *Methods mol Biol*. 2013;1018:93–104. PMID: 23681620.
106. Wewetzer K, Radtke C, Kocsis J, Baumgartner W. Species-specific control of cellular proliferation and the impact of large animal models for the use of olfactory ensheathing cells and Schwann cells in spinal cord repair. *Exp Neurol*. 2011;229:80–87. [PMID: 20816827]. doi:10.1016/j.expneurol.2010.08.029
107. Huang H, Winter EE, Wang H, et al. Evolutionary conservation and selection of human disease gene orthologs in the rat and mouse genomes. *Genome Biol*. 2004;5:R47. [PMID: 15239832]. doi:10.1186/gb-2004-5-7-r47
108. Wright SN, Leger BS, Rosenthal SB, et al. Genome-wide association studies of human and rat BMI converge on synapse, epigenome, and hormone signaling networks. *Cell Rep*. 2023;42:112873. [PMID: 37527041]. doi:10.1016/j.celrep.2023.112873
109. Conner JM, Franks KM, Titterness AK, et al. NGF is essential for hippocampal plasticity and learning. *J Neurosci*. 2009;29:10883–10889. [PMID: 19726646]. doi:10.1523/JNEUROSCI.2594-09.2009
110. Guo L, Yeh ML, Cuzon Carlson VC, Johnson-Venkatesh EM, Yeh HH. Nerve growth factor in the hippocamposeptal system: evidence for activity-dependent anterograde delivery and modulation of synaptic activity. *J Neurosci*. 2012;32:7701–7710. [PMID: 22649248]. doi:10.1523/JNEUROSCI.0028-12.2012
111. Cong M, Shen M, Wu X, et al. Improvement of sensory neuron growth and survival via negatively regulating PTEN by miR-21-5p-contained small extracellular vesicles from skin precursor-derived Schwann cells. *Stem Cell Res Ther*. 2021;12:80. [PMID: 33494833]. doi:10.1186/s13287-020-02125-4
112. Kar AN, Lee SJ, Sahoo PK, et al. MicroRNAs 21 and 199a-3p regulate axon growth potential through modulation of Pten and mTor mRNAs. *eNeuro*. 2021;8:ENEURO.0155–21.2021. [PMID: 34326064]. doi:10.1523/ENEURO.0155-21.2021
113. Liu R, Wang W, Wang S, Xie W, Li H, Ning B. microRNA-21 regulates astrocytic reaction post-acute phase of spinal cord injury through modulating TGF-beta signaling. *Aging*. 2018;10:1474–1488. [PMID: 29936495]. doi:10.18632/aging.101484
114. Sun T, Duan L, Li J, Guo H, Xiong M. Gypenoside XVII protects against spinal cord injury in mice by regulating the microRNA-21-mediated PTEN/AKT/mTOR pathway. *Int J Mol Med*. 2021;48:146. [PMID: 34132355]. doi:10.3892/ijmm.2021.4979
115. Araki W, Wurtman RJ. Control of membrane phosphatidylcholine biosynthesis by diacylglycerol levels in neuronal cells undergoing neurite outgrowth. *Proc Natl Acad Sci U S A*. 1997;94:11946–11950. [PMID: 9342342]. doi:10.1073/pnas.94.22.11946
116. Yang C, Wang X, Wang J, et al. Rewiring neuronal glycerolipid metabolism determines the extent of axon regeneration. *Neuron*. 2020;105(2):276–292e5. [PMID: 31786011]. doi:10.1016/j.neuron.2019.10.009
117. Harel R, Futerman AH. Inhibition of sphingolipid synthesis affects axonal outgrowth in cultured hippocampal neurons. *J Biol Chem*. 1993;268:14476–14481. [PMID: 8314804]. doi:10.1016/S0021-9258(19)85263-8
118. Hussain G, Wang J, Rasul A, et al. Role of cholesterol and sphingolipids in brain development and neurological diseases. *Lipids Health Dis*. 2019;18:26. [PMID: 30683111]. doi:10.1186/s12944-019-0965-z
119. Olsen ASB, Faergeman NJ. Sphingolipids: membrane microdomains in brain development, function and neurological diseases. *Open Biol*. 2017;7:170069. [PMID: 28566300]. doi:10.1098/rsob.170069
120. Schwarz A, Rapaport E, Hirschberg K, Futerman AH. A regulatory role for sphingolipids in neuronal growth. Inhibition of sphingolipid synthesis and degradation have opposite effects on axonal branching. *J Biol Chem*. 1995;270:10990–10998. [PMID: 7738041]. doi:10.1074/jbc.270.18.10990
121. Aoi W, Tanimura Y. Roles of skeletal muscle-derived exosomes in organ metabolic and immunological communication. *Front Endocrinol*. 2021;12:697204. [PMID: 34594301]. doi:10.3389/fendo.2021.697204
122. De Gasperi R, Hamidi S, Harlow LM, Ksiezak-Reding H, Bauman WA, Cardozo CP. Denervation-related alterations and biological activity of miRNAs contained in exosomes released by skeletal muscle fibers. *Sci Rep*. 2017;7:12888. [PMID: 29038428]. doi:10.1038/s41598-017-13105-9
123. Blaya M O, Pressman Y, Andreu M, Moreno W J, Sanchez-Molano J, Kerr N A, Umland O, Khan A, Bramlett H M, Dietrich W Dalton. (2025). Human Schwann cell exosome treatment attenuates secondary injury mechanisms, histopathological consequences, and behavioral deficits after traumatic brain injury. Neurotherapeutics, e00555 PMID: 39988499 10.1016/j.neurot.2025.e00555
124. Ge XT, Lei P, Wang HC, et al. miR-21 improves the neurological outcome after traumatic brain injury in rats. *Sci Rep*. 2014;4:6718. [PMID: 25342226]. doi:10.1038/srep06718
125. Chen Q, Xu J, Li L, et al. MicroRNA-23a/b and microRNA-27a/b suppress Apaf-1 protein and alleviate hypoxia-induced neuronal apoptosis. *Cell Death Dis*. 2014;5:e1132. [PMID: 24651435]. doi:10.1038/cddis.2014.92
126. Wang W, Liu R, Su Y, Li H, Xie W, Ning B. MicroRNA-21-5p mediates TGF-beta-regulated fibrogenic activation of spinal fibroblasts and the formation of fibrotic scars after spinal cord injury. *Int J Biol Sci*. 2018;14:178–188. [PMID: 29483836]. doi:10.7150/ijbs.24074
127. Wang Y, Han T, Guo R, et al. Micro-RNA let-7a-5p derived from mesenchymal stem cell-derived extracellular vesicles promotes the regrowth of neurons in spinal-cord-injured rats by targeting the HMGA2/SMAD2 axis. *Front Mol Neurosci*. 2022;15:850364. [PMID: 35401112]. doi:10.3389/fnmol.2022.850364
128. Cheng PH, Li CL, Chang YF, et al. miR-196a ameliorates phenotypes of Huntington disease in cell, transgenic mouse, and induced pluripotent stem cell models. *Am J Hum Genet*. 2013;93:306–312. [PMID: 23810380]. doi:10.1016/j.ajhg.2013.05.025
129. Liguori M, Nuzziello N, Introna A, et al. Dysregulation of microRNAs and target genes networks in peripheral blood of patients with sporadic amyotrophic lateral sclerosis. *Front Mol Neurosci*. 2018;11:288. [PMID: 30210287]. doi:10.3389/fnmol.2018.00288
130. Xiang W, Jiang L, Zhou Y, et al. The lncRNA Ftx/miR-382-5p/Nrg1 axis improves the inflammation response of microglia and spinal cord injury repair. *Neurochem Int*. 2021;143:104929. [PMID: 33359189]. doi:10.1016/j.neuint.2020.104929